Supplemental Information for:

Tunable Electronic Coupling in Linked Bis(cubane) Cobalt-Oxo Clusters

Table of Contents

General considerations: Cobalt(II) nitrate hexahydrate, cobalt(II) acetate tetrahydrate, pyridine, hydrogen peroxide (34-37% in water), 4-methylpyridine, 4-methoxypyridine, 4-cyanopyridine, 4-N,N-dimethylaminopyridine, pyrazine, 4,4'-bipyridine, lithium benzoate, 4-chlorobenzoic acid, 4-methoxybenzoic acid, 3,4,5-(trimethoxy)benzoic acid, and tetrabutylammonium bromide were purchased from Sigma-Aldrich and used without further purification. Lithium tetrakis(pentafluorophenyl)borate was purchased from Boulder Scientific Company and used without further purification. Solvents were purchased from Fisher-Scientific and used without any further purification. The complexes $Co_4O_4(OAc)_4$(4-methylpyridine)$_4$,[1] $Co_4O_4(OAc)_4$(4-cyanopyridine)$_4$,[1] $Co_4O_4(OAc)_4$(4-methoxypyridine)$_4$,[2] $Co_4O_4(OAc)_4$(4-N,N-dimethylaminopyridine)$_4$,[2] $Co_4O_4(OBz)_4$(4-methylpyridine)$_4$,[3] $Co_4O_4(OBz)_4$(4-methoxypyridine)$_4$,[3] Co_4O_4(4-methoxybenzoate)$_4$(4-methoxypyridine)$_4$[3], and Co_4O_4(3,4,5-(trimethoxy)benzoate)$_4$(4-methoxypyridine)$_4$[3] were prepared according to previously published literature procedures. Electrochemical grade tetrabutylammonium tetrakis(pentafluorophenyl)borate was prepared and crystalized according to published literature procedures.[4] The synthetic procedures described below were conducted in air.

Analytical Methods: Element analyses were performed at the Microanalytical Laboratory at the University of California, Berkeley or at CENTC Elemental Analysis Facility at the University of Rochester, using a Perkin Elmer 2400 Series II combustion analyzer equipped for determination of %C, %H, and %N. High-resolution electrospray ionization mass spectrometry (HR-ESI-MS) measurements were performed using a Perkin Elmer AxION 2 TOF Spectrometer at the Catalysis Center at UC Berkeley.

Routine NMR spectra were recorded on a Bruker AV-500 spectrometer at room temperature. CD_2Cl_2 and methanol-d_4 were purchased from Cambridge Isotope Laboratories. ^{1}H NMR spectra were referenced to residual protio-solvent peak (δ 5.32 for CD_2Cl_2, δ 3.31 for methanol-d_4). All spectra were recorded in 5% methanol-d_4 in CD_2Cl_2 except for MePy-OAc-bipy which was recoded in methanol-d_4.

Electrochemical experiments were performed at 292 K in atmosphere using a BASi EC Epsilon potentiostat/galvanostat and a PWR-3 Power Module. Measurements were collected with a three-electrode setup with a 3 mm diameter glassy carbon working electrode, Pt wire auxiliary electrode, and Ag wire floating reference. The working electrode was polished with 0.30 μm alumina slurries, followed by additional 0.05 μm alumina slurries, rinsed with water, and dried in atmosphere before use. Electrochemical grade tetrabutylammonium hexafluorophosphate (0.25 M) or tetrabutylammonium (tetrakis)pentafluorophenyl)borate (0.1 M) was used as the electrolyte. Analyte concentration was 1.0 mM in CH_2Cl_2. All reported values of E_1 and E_2 are the local current maxima observed by DPV. The peak currents were determined by EC Lab software. Ferrocene (Cp_2Fe) was added at the end of each experiment as an internal reference against the half-potential of the $[Cp_2Fe]^0$ /$[Cp_2Fe]^+$ redox couple. Spectroelectrochemical measurements were recorded on Cary 5000 UV-Vis-NIR spectrometer with a Pines Research platinum honeycomb cell with a silver wire pseudoreference electrode.

Synthetic Procedures

($Co_4O_4(OAc)_4$(4-Methylpyridine)$_2$(μ-4,4'-Bipyridyl))$_2$ (MePy-OAc-bipy). $Co_4O_4(OAc)_4$(4-methylpyridine)$_4$ (1.00 g, 1.1 mmol, 1 equiv) was added to a 1L three-neck round-bottom flask, followed by acetonitrile (400 mL) equipped with a magnetic stir bar, reflux condenser, glass stopper, and a rubber septum and the reaction vessel was lowered into an oil bath heated to 90 ˚C and the solution allowed to come to reflux. Subsequently, 4,4'-bipyridyl (0.172 g, 1.1 mmol, 1 eq) was dissolved in 20 mL acetonitrile and loaded into a 24 mL syringe. The syringe containing the 4,4'-biyridyl solution was fitted to a syringe pump and positioned with needle to deliver its contents into the three-neck round-bottom flask through the rubber septum. The syringe pump was programed to deliver its contents at a rate of 4 mL/h, delivering the entire 4,4'-bipyridyl solution over the course of 5 hours by which point a gradual color change from green to red could be observed. The reaction was heated for a further 11 hours. The resulting red solution was evaporated to dryness becoming more vibrant in color upon drying. The resultant red solids were loaded onto a silica-gel column and eluted with 7.5% methanol in dichloromethane. The product was further purified by crystallization from a dichloromethane solution layered with hexanes to obtain a rust-red solid (318.8 mg, 33%). ^{1}H NMR (500 MHz, MeOD) δ 8.53 (d, *J* = 6.1 Hz, 8H), 8.16 (d, *J* = 5.6 Hz, 8H), 7.66 (d, *J* = 6.8 Hz, 8H), 6.97 (d, *J* = 5.6 Hz, 8H), 2.32 (s, 12H), 2.06 (s, 24H). ^{13}C NMR (126 MHz, MeOD) δ 187.08, 153.73, 152.13, 149.74, 144.96, 124.79, 121.41, 25.04, 19.53. Anal. Calcd. For $C_{60}H_{68}Co_8N_8O_{24}$: C, 41.02; H, 3.90; N, 6.38. Found: C, 40.53; H, 3.94; N, 6.95. (ESI): Calcd for $[C_{60}H_{69}Co_8N_8O_{24}]^+$: *m/z* = 1756.90. Found: *m/z* = 1756.87

($Co_4O_4(OAc)_4$(4-Methylpyridine)$_2$(μ-pyrazine))$_2$ (MePy-OAc). $Co_4O_4(OAc)_4$(4-methylpyridine)$_4$ (1.00 g, 1.10 mmol, 1 equiv), pyrazine (0.4408 g, 5.51 mmol, 5 equiv.) and 150 mL acetonitrile were added to a 500 mL pressure vessel equipped with a magnetic stir bar and the vessel was tightly sealed. The reaction vessel was lowered into an oil bath heated to 80 ˚C and heated for 16 h by which point a green to red color change could be observed alongside the formation of a red precipitate. The reaction vessel was allowed to cool to room temperature before opening. The mixture was filtered through a pad of Celite® and the resulting red solids were washed with acetonitrile (100 mL x 3). The product was washed from the filter with dichloromethane. The product was further purified by crystallization from a dichloromethane solution layered with hexanes to obtain a rust-red solid (407.4 mg, 46%). ^{1}H NMR (500 MHz, CD_2Cl_2) δ 8.70 (s, 8H), 8.27 (d, *J* = 6.4 Hz, 8H), 6.97 (d, *J* = 6.4 Hz, 8H), 2.37 (s, 12H), 2.15 (s, 24H). Anal. Calcd. For $C_{48}H_{60}Co_8N_8O_{24}$: C, 35.93; H, 3.77; N, 6.98. Found: C, 35.48; H, 3.89; N, 6.52. (ESI): Calcd for $[C_{48}H_{61}Co_8N_8O_{24}]^+$: *m/z* = 1604.85. Found: *m/z* = 1604.84

($Co_4O_4(OAc)_4$(4-Methoxypyridine)$_2$(μ-pyrazine))$_2$ (MeOPy-OAc). $Co_4O_4(OAc)_4$(4-methoxypyridine)$_4$ (0.500 g, 0.514 mmol, 1 equiv), pyrazine (0.1647 g, 2.056 mmol, 4 equiv.) and 75 mL acetonitrile were added to a 125 mL pressure vessel equipped with a magnetic stir bar and the vessel was tightly sealed. The reaction vessel was lowered into an oil bath heated to 80 ˚C and heated for 16 h by which point a green to red color change could be observed alongside the formation of a red precipitate. The reaction vessel was allowed to cool to room temperature before opening. The mixture was filtered through a pad of Celite® and the resulting red solids

were washed with acetonitrile (50 mL x 3). The product was washed from the filter with a 1:1 mixture of methanol:dichloromethane. The resulting solution was concentrated to obtain a rust-red powder (407.4 mg, 57%). ^{1}H NMR (500 MHz, CD_2Cl_2) δ 8.69 (s, 8H), 8.22 (d, J = 6.7 Hz, 8H), 6.70 (d, J = 6.9 Hz, 8H), 3.88 (s, 12H), 2.16 (s, 24H). ^{13}C NMR (126 MHz, CD_2Cl_2) δ 187.22, 166.91, 153.59, 148.58, 110.40, 55.63, 26.30. Anal. Calcd. For $C_{48}H_{60}Co_8N_8O_{28}$: C, 34.55; H, 3.62; N, 6.72. Found: C, 34.44; H, 3.15; N, 6.71.

$(Co_4O_4(OAc)_4$(4-N,N-Dimethylaminopyridine)$_2$(μ-pyrazine))$_2$ (DMAP-OAc). $Co_4O_4(OAc)_4$(4-N,N-dimethylaminopyridine)$_4$ (0.250 g, 0.244 mmol, 1 equiv), pyrazine (0.07816 g, 0.976 mmol, 4 equiv.) and 50 mL tetrahydrofuran were added to a 100 mL pressure vessel equipped with a magnetic stir bar and the vessel was tightly sealed. The reaction vessel was lowered into an oil bath heated to 75 ˚C and heated for 16 h by which point a green to red color change could be observed alongside the formation of a red precipitate. The reaction vessel was allowed to cool to room temperature before opening. The mixture was filtered through a pad of Celite® and the resulting red solids were washed with tetrahydrofuran (30 mL x 3). The product was washed from the filter with dichloromethane. The product was further purified by crystallization from a dichloromethane solution layered with hexanes to obtain a rust-red solid (63.46 mg, 30%). ^{1}H NMR (500 MHz, CD_2Cl_2) δ 8.70 (s, 8H), 7.92 (d, J = 7.0 Hz, 8H), 6.35 (d, J = 7.2 Hz, 8H), 3.02 (s, 24H), 2.14 (s, 24H). ^{13}C NMR (126 MHz, CD_2Cl_2) δ 186.87, 154.58, 151.27, 148.52, 107.04, 107.01, 38.97, 26.29. Anal. Calcd. For $C_{52}H_{72}Co_8N_{12}O_{24}$: C, 36.30; H, 4.22; N, 9.77. Found: C, 36.40; H, 3.84; N, 9.51.

$(Co_4O_4$(Benzoate)$_4$(4-Methoxypyridine)$_2$(μ-pyrazine))$_2$ (MeOPy-BzO). Co_4O_4(benzoate)$_4$(4-methoxypyridine)$_4$ (0.100 g, 0.082 mmol, 1 equiv), pyrazine (0.0197 g, 0.246 mmol, 3 equiv.) and 15 mL acetonitrile were added to a 20 mL screw-cap glass vial equipped with a magnetic stir bar and the vessel was tightly sealed. The reaction vessel was lowered into an oil bath heated to 80 ˚C and heated for 16 h by which point a green to red color change could be observed alongside the formation of a red precipitate. The reaction vessel was allowed to cool to room temperature before opening. The mixture was filtered through a pad of Celite® and the resulting red solids were washed with acetonitrile (5 mL x 3). The product was washed from the filter with dichloromethane and the resultant solution was loaded onto a silica gel column. The product was eluted using 2.5% acetone and 0.25% methanol in dichloromethane and concentrated to a red powder (14.1 mg, 16%). ^{1}H NMR (500 MHz, CD_2Cl_2) δ 8.86 (s, 8H), 8.33 (d, J = 7.0 Hz, 8H), 8.02 (d, J = 7.0 Hz, 16H), 7.44 (t, J = 7.4 Hz, 8H), 7.33 (t, J = 7.7 Hz, 16H), 6.67 (d, J = 7.0 Hz, 8H), 3.85 (s, 12H). ^{13}C NMR (126 MHz, CD_2Cl_2) δ 181.06, 166.87, 153.84, 149.05, 135.39, 131.26, 128.99, 127.64, 110.47, 55.60. Anal. Calcd. For $C_{88}H_{76}Co_8N_8O_{28}$: C, 48.82; H, 3.54; N, 5.18. Found: C, 49.00; H, 3.69; N, 5.08.

$(Co_4O_4$(4-Methoxybenzoate)$_4$(4-Methoxypyridine)$_2$(μ-pyrazine))$_2$ (MeOPy-MeOBzO). Co_4O_4(4-methoxybenzoate)$_4$(4-methoxypyridine)$_4$ (0.300 g, 0.224 mmol, 1 equiv), pyrazine

(0.0541 g, 0.676 mmol, 3 equiv.) and 45 mL acetonitrile were added to a 100 mL pressure vessel equipped with a magnetic stir bar and the vessel was tightly sealed. The reaction vessel was lowered into an oil bath heated to 80 ˚C and heated for 16 h by which point a green to red color change could be observed alongside the formation of a red precipitate. The reaction vessel was allowed to cool to room temperature before opening. The mixture was filtered through a pad of Celite® and the resulting red solids were washed with acetonitrile (15 mL x 3). The product was washed from the filter with dichloromethane and the resultant solution was loaded onto a silica gel column. The product was eluted using 5% acetone and 0.5% methanol in dichloromethane and concentrated to a red powder (26.3 mg, 9.6%). ^{1}H NMR (500 MHz, CD_2Cl_2) δ 8.81 (s, 8H), 8.33 (d, *J* = 7.0 Hz, 8H), 7.96 (d, *J* = 8.9 Hz, 16H), 6.82 (d, *J* = 8.9 Hz, 16H), 6.63 (d, *J* = 7.2 Hz, 8H), 3.84 (s, 12H), 3.81 (s, 24H). ^{13}C NMR (126 MHz, CD_2Cl_2) δ 180.53, 166.74, 162.15, 153.83, 148.85, 130.83, 128.44, 112.70, 110.28, 55.57, 55.27. Anal. Calcd. For $C_{96}H_{92}Co_8N_8O_{36}$: C, 47.90; H, 3.86; N, 4.66. Found: C, 48.30; H, 3.28; N, 4.41.

(Co_4O_4(3,4,5-(Trimethoxy)benzoate)$_4$(4-Methoxypyridine)$_2$(μ-pyrazine))$_2$ (MeOPy-(MeO)$_3$BzO). Co_4O_4(3,4,5-(trimethoxy)benzoate)$_4$(4-methoxypyridine)$_4$ (0.100 g, 0.063 mmol, 1 equiv), pyrazine (0.0252 g, 0.315 mmol, 5 equiv.) and 15 mL acetonitrile were added to a 20 mL screw-cap glass vial equipped with a magnetic stir bar and the vessel was tightly sealed. The reaction vessel was lowered into an oil bath heated to 80 ˚C and heated for 16 h by which point a green to red color change could be observed alongside the formation of a red precipitate. The reaction vessel was allowed to cool to room temperature before opening. The mixture was filtered through a pad of Celite® and the resulting red solids were washed with acetonitrile (5 mL x 3). The product was washed from the filter with dichloromethane and the resultant solution was loaded onto a silica gel column. The product was eluted using 15% acetone and 1.5% methanol in dichloromethane and concentrated to a red powder (13.1 mg, 14%). ^{1}H NMR (500 MHz, CD_2Cl_2) δ 8.84 (s, 8H), 7.29 (s, 16H), 6.63 (d, *J* = 7.0 Hz, 8H), 3.84 (s, 12H), 3.78 (s, 24H), 3.78 (s, 28H). ^{13}C NMR (126 MHz, CD_2Cl_2) δ 180.25, 166.88, 153.85, 152.50, 149.03, 141.44, 130.80, 110.27, 106.84, 60.47, 56.22, 55.62. Anal. Calcd. For $C_{112}H_{124}Co_8N_8O_{52}$: C, 46.60; H, 4.33; N, 3.88. Found: C, 47.50; H, 4.28; N, 3.83.

(Co_4O_4(Benzoate)$_4$(4-Methylpyridine)$_2$(μ-pyrazine))$_2$ (MePy-BzO). MePy-OAc (0.100 g, 0.062 mmol, 1 equiv), benzoic acid (0.0913 g, 0.748 mmol, 12 equiv.) and 10 mL methanol were added to a 20 mL screw-cap glass vial equipped with a magnetic stir bar and the vessel was tightly sealed. The reaction vessel was lowered into an oil bath heated to 70 ˚C and heated for 16 h by which point the formation of a red precipitate could be observed. The reaction vessel was allowed to cool to room temperature before opening. The mixture was filtered through a pad of Celite® and the resulting red solids were washed with methanol (5 mL x 3) and acetonitrile (5 mL x 3). The product was washed from the filter with dichloromethane and the resultant solution was loaded onto a silica gel column. The product was eluted using 5% acetone and 0.5% methanol in dichloromethane and concentrated to a red powder (20.2 mg, 16%). ^{1}H NMR (500 MHz, CD_2Cl_2) δ 8.86 (s, 8H), 8.39 (d, *J* = 6.4 Hz, 8H), 8.00 (d, *J* = 7.0 Hz, 16H), 7.43 (t, *J* = 7.4 Hz,

8H), 7.32 (t, J = 7.7 Hz, 16H), 6.93 (d, J = 7.2 Hz, 8H), 2.35 (s, 12H). ^{13}C NMR (126 MHz, CD_2Cl_2) δ 180.94, 152.42, 148.99, 135.46, 131.23, 128.99, 127.64, 124.78, 20.59. Anal. Calcd. For $C_{88}H_{76}Co_8N_8O_{24}$: C, 50.31; H, 3.65; N, 5.33. Found: C, 51.40; H, 3.98; N, 4.85.

(Co_4O_4(4-Chlorobenzoate)$_4$(4-Methylpyridine)$_2$(μ-pyrazine))$_2$ (MePy-ClBzO). MePy-OAc (0.150 g, 0.093 mmol, 1 equiv), 4-chlorobenzoic acid (0.1756 g, 1.122 mmol, 12 equiv.) 5 mL methanol and 5 mL acetonitrile were added to a 20 mL screw-cap glass vial equipped with a magnetic stir bar and the vessel was tightly sealed. The reaction vessel was lowered into an oil bath heated to 70 ˚C and heated for 16 h by which point the formation of a red precipitate could be observed. The reaction vessel was allowed to cool to room temperature before opening. The mixture was filtered through a pad of Celite® and the resulting red solids were washed with methanol (5 mL x 3) and acetonitrile (5 mL x 3). The product was washed from the filter with dichloromethane and the resultant solution was loaded onto a silica gel column. The product was eluted using 2.5% acetone and 0.25% methanol in dichloromethane and concentrated to a red powder (49.3 mg, 22%). ^{1}H NMR (500 MHz, CD_2Cl_2) δ 8.81 (s, 1H), 8.33 (d, J = 5.6 Hz, 1H), 7.95 (d, J = 8.5 Hz, 1H), 7.31 (d, J = 8.5 Hz, 1H), 6.92 (d, J = 5.6 Hz, 1H), 2.36 (s, 1H). ^{13}C NMR (126 MHz, CD_2Cl_2) δ 179.91, 152.25, 148.87, 137.52, 133.80, 130.48, 127.92, 124.87, 20.63. Anal. Calcd. For $C_{88}H_{68}Cl_8Co_8N_8O_{24}$: C, 44.47; H, 2.88; N, 4.71. Found: C, 43.81; H, 3.27; N, 4.38.

NMR Spectra

MePy-OAc-bipy

^{1}H-NMR

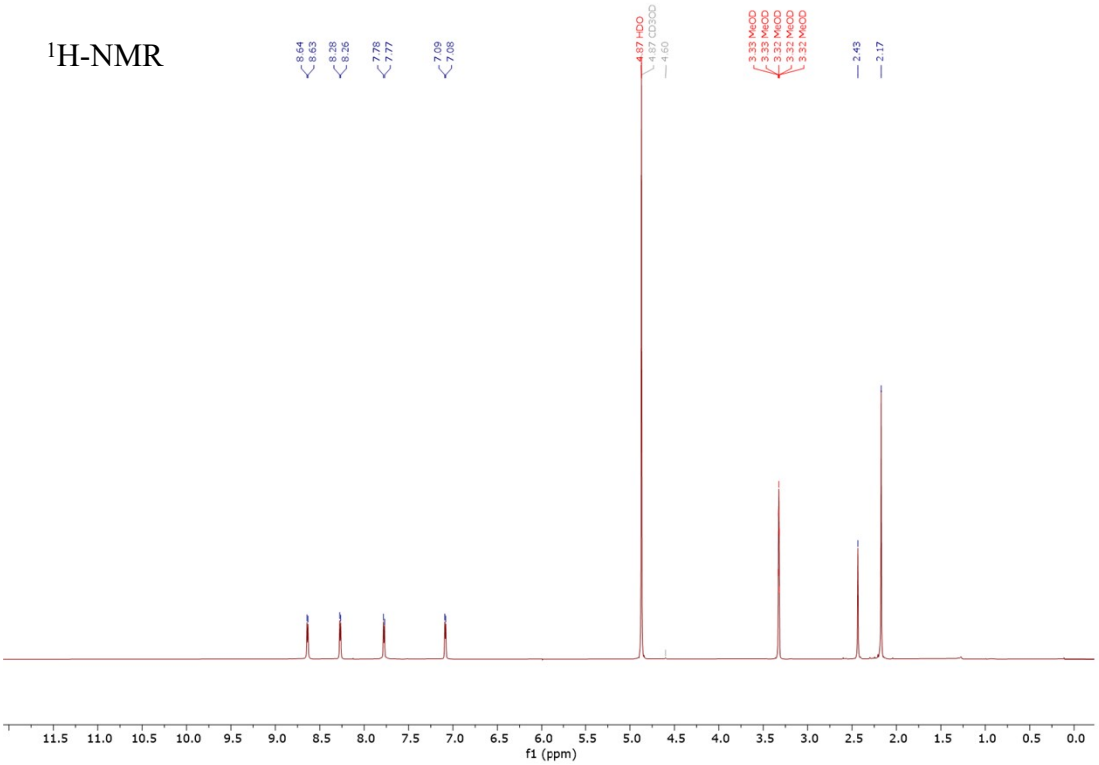

^{13}C-NMR

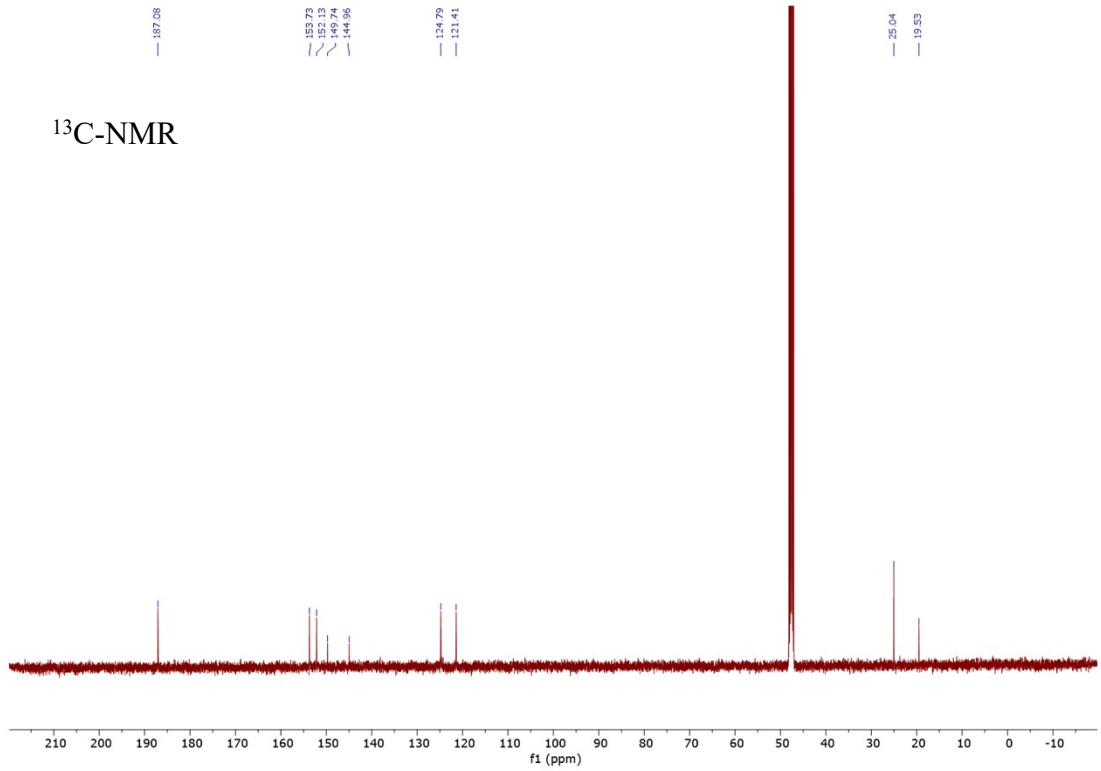

MePy-OAc

^{1}H-NMR

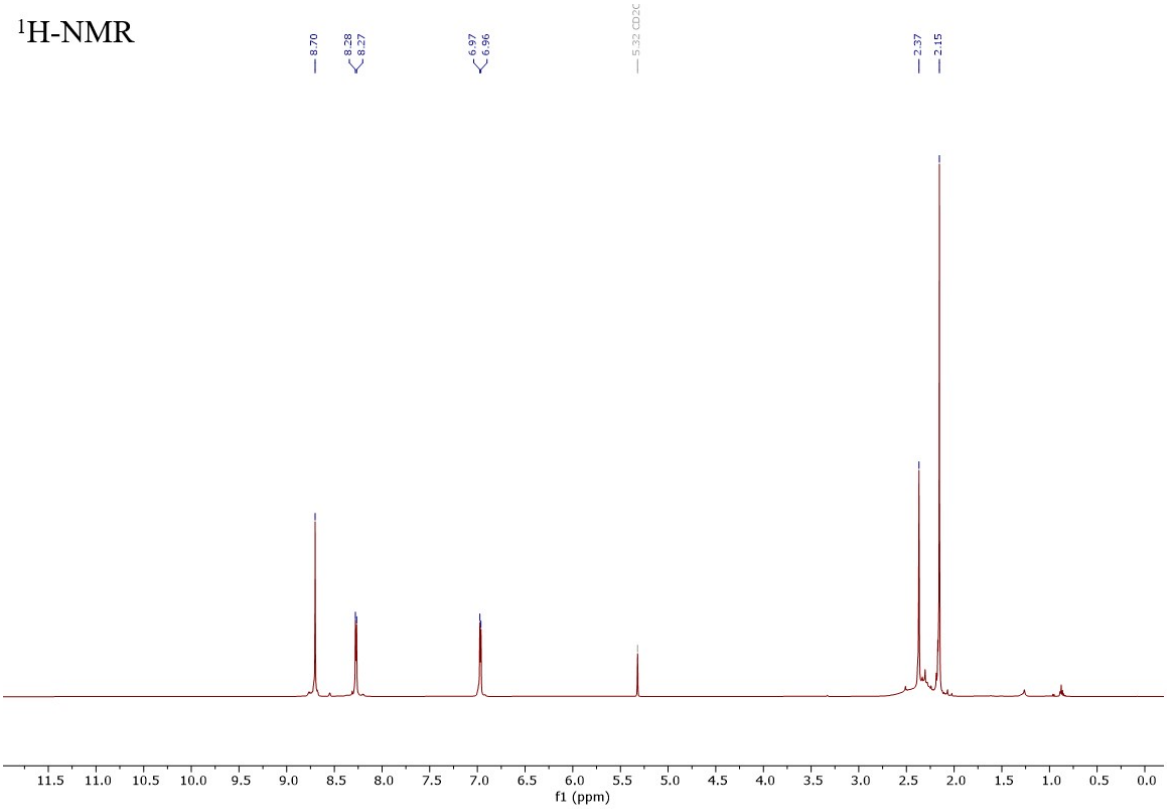

^{13}C-NMR

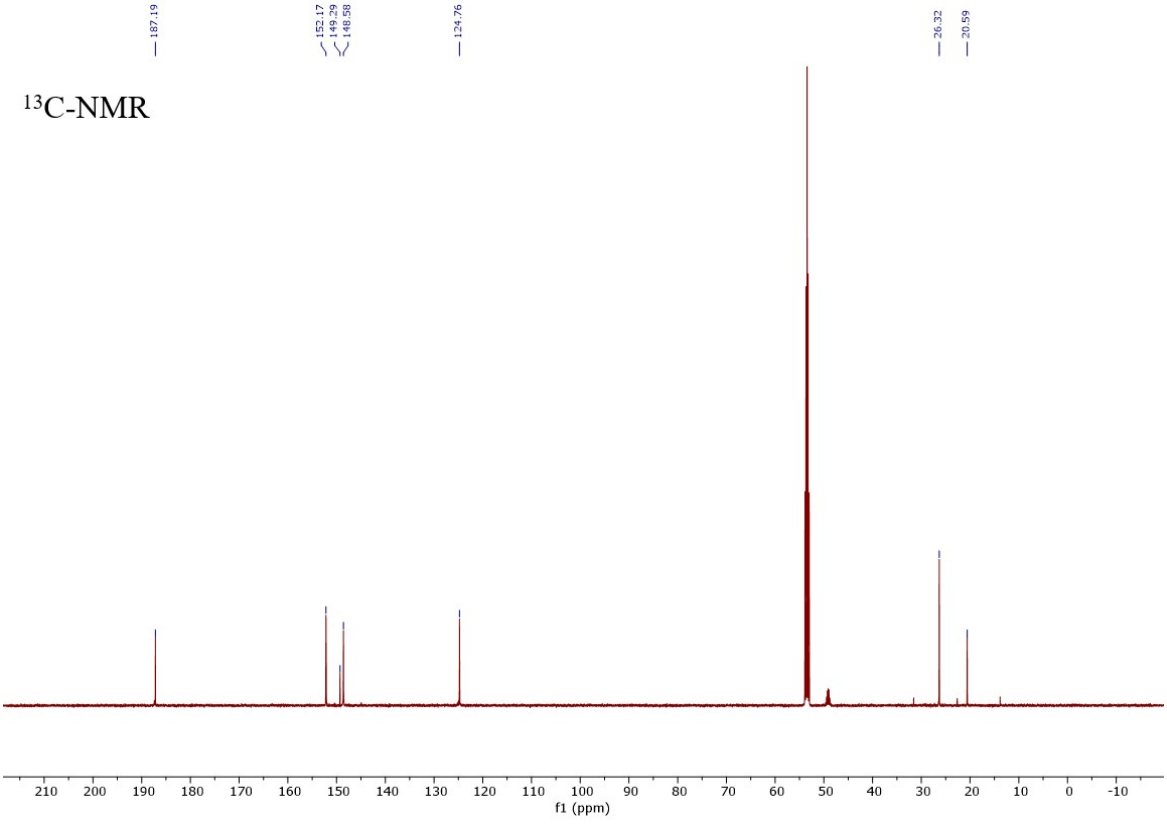

MeOPy-OAc

^{1}H-NMR

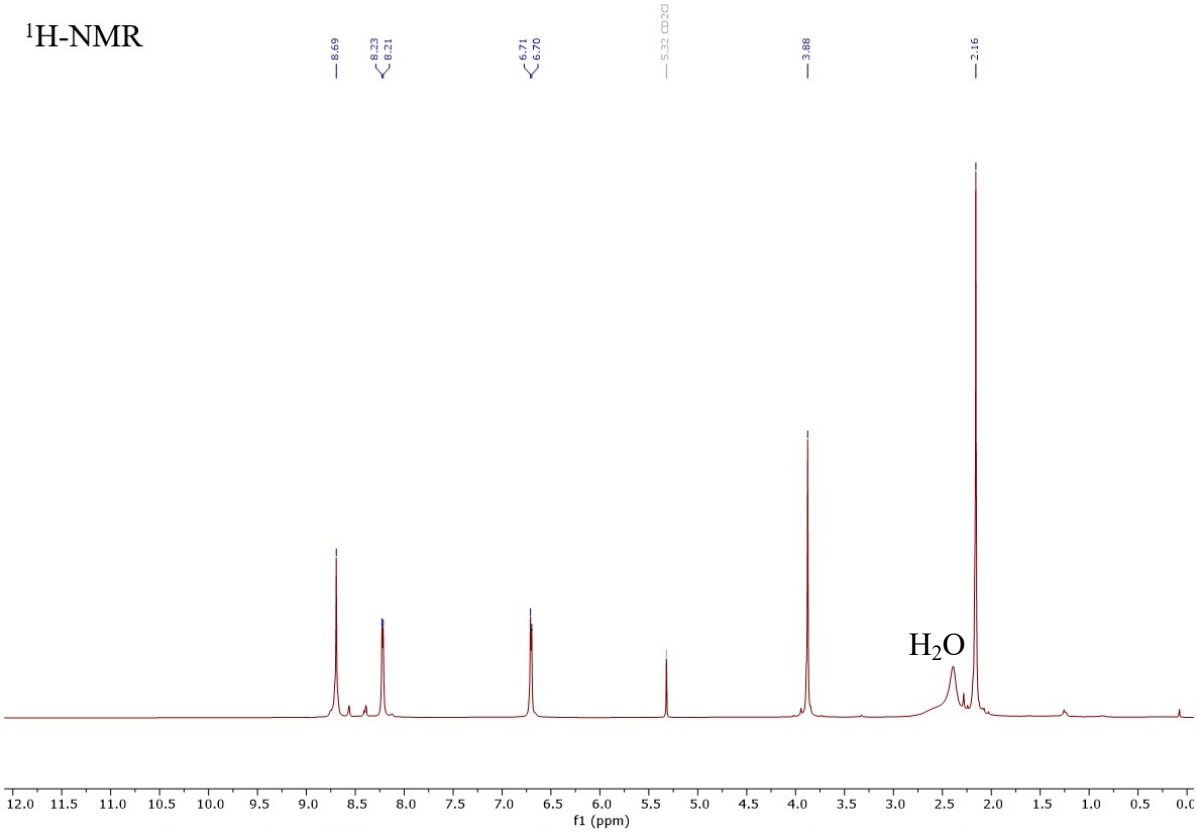

^{13}C-NMR

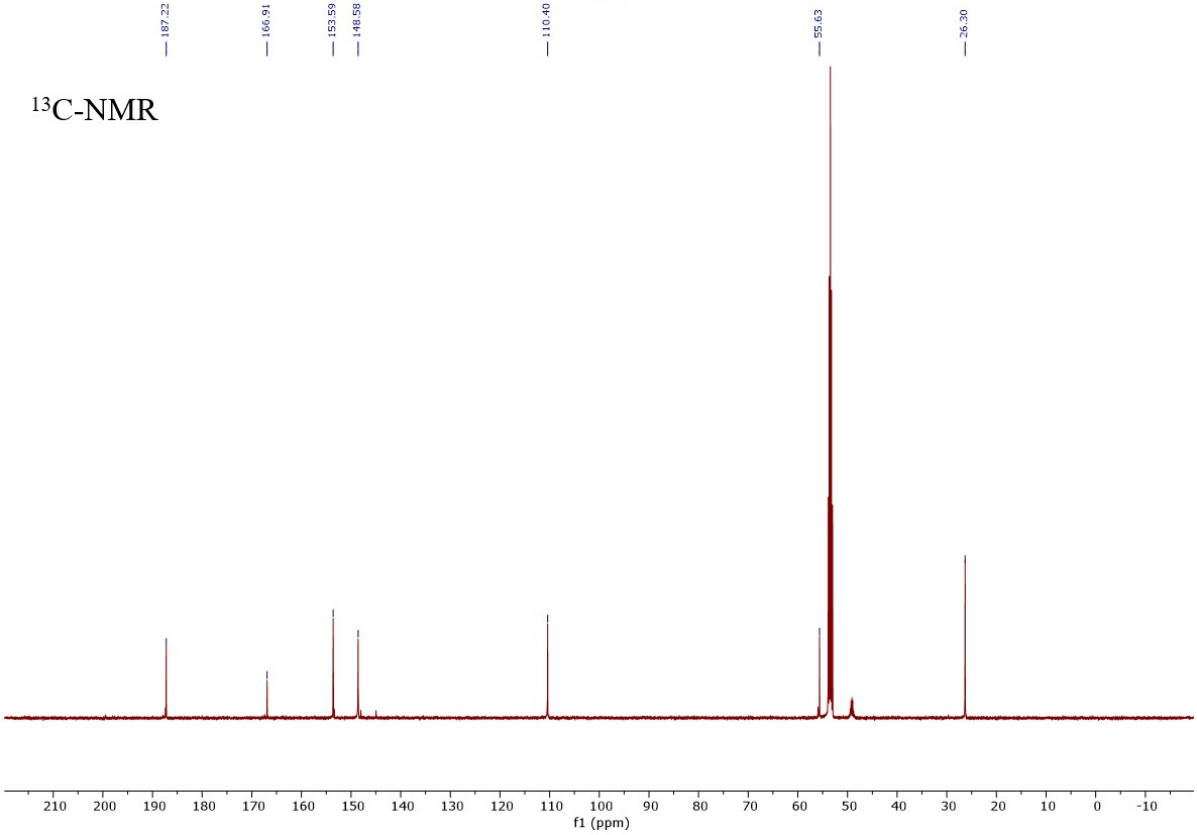

DMAP-OAc

^{1}H-NMR

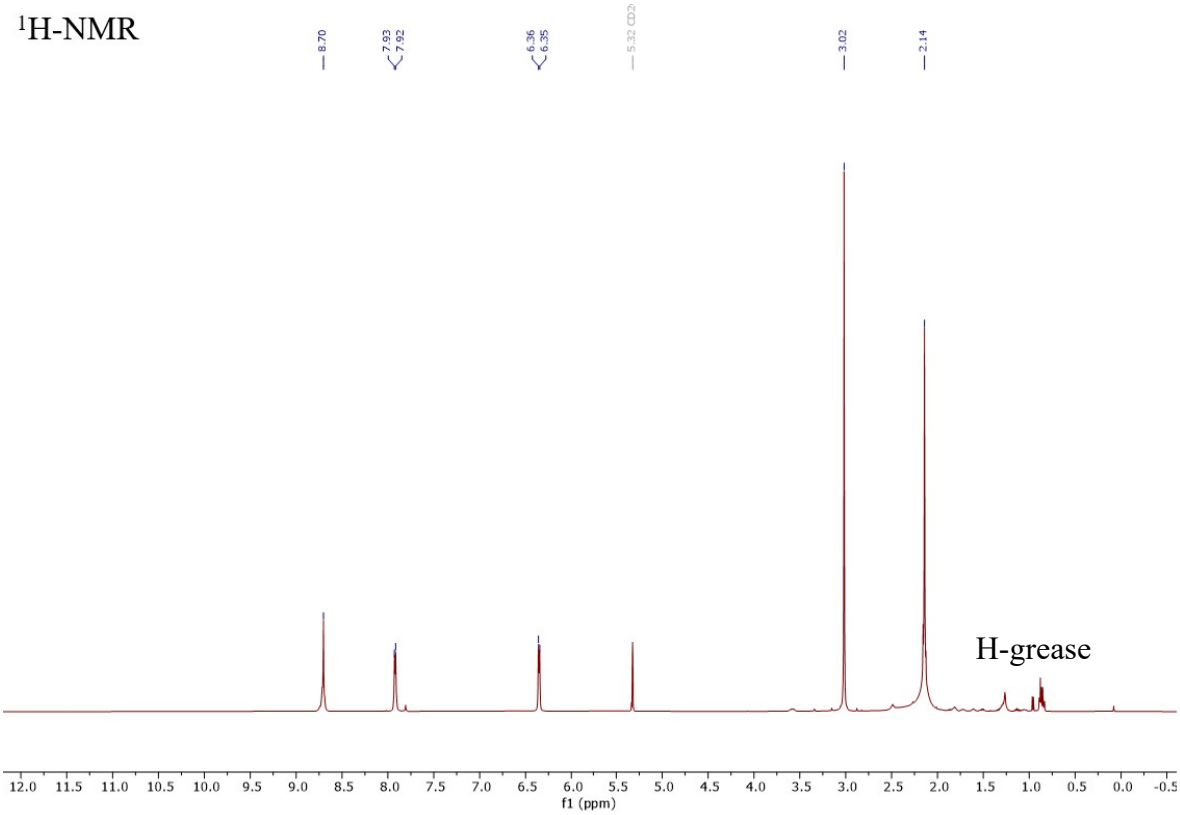

^{13}C-NMR

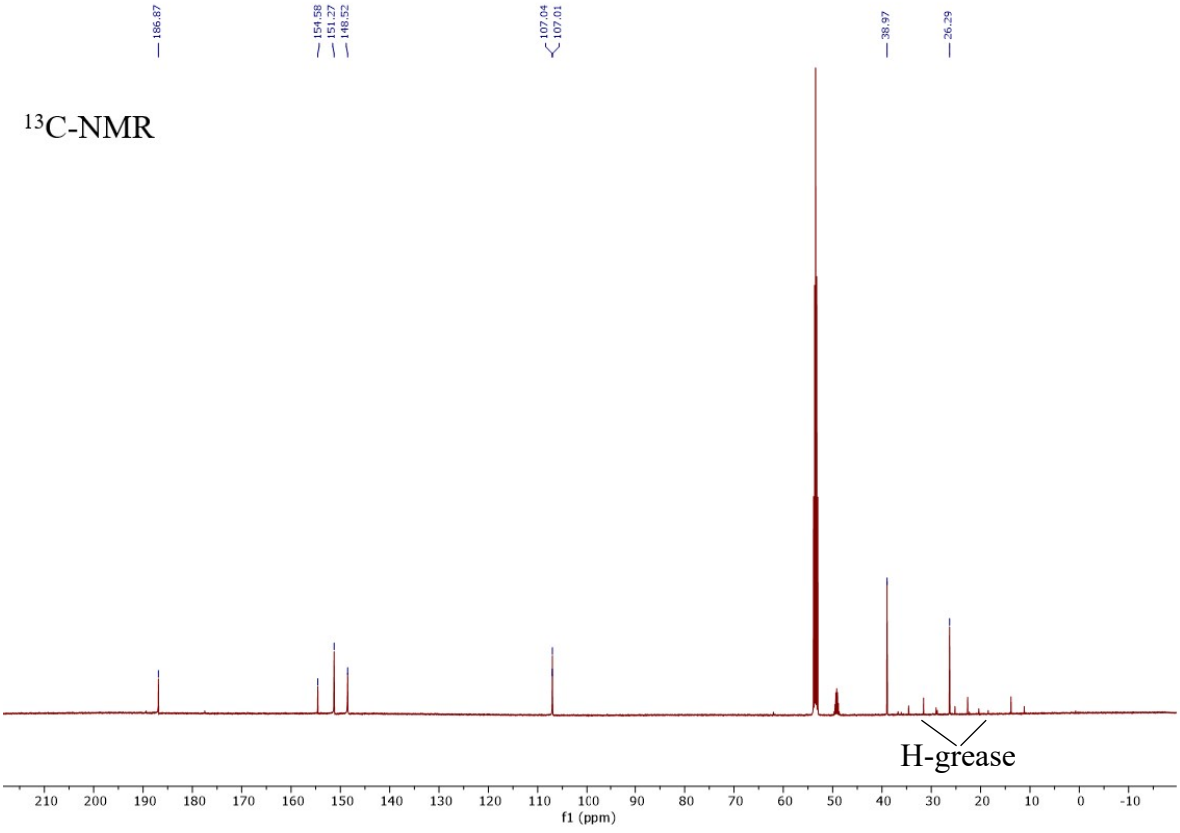

MeOPy-BzO

^{1}H-NMR

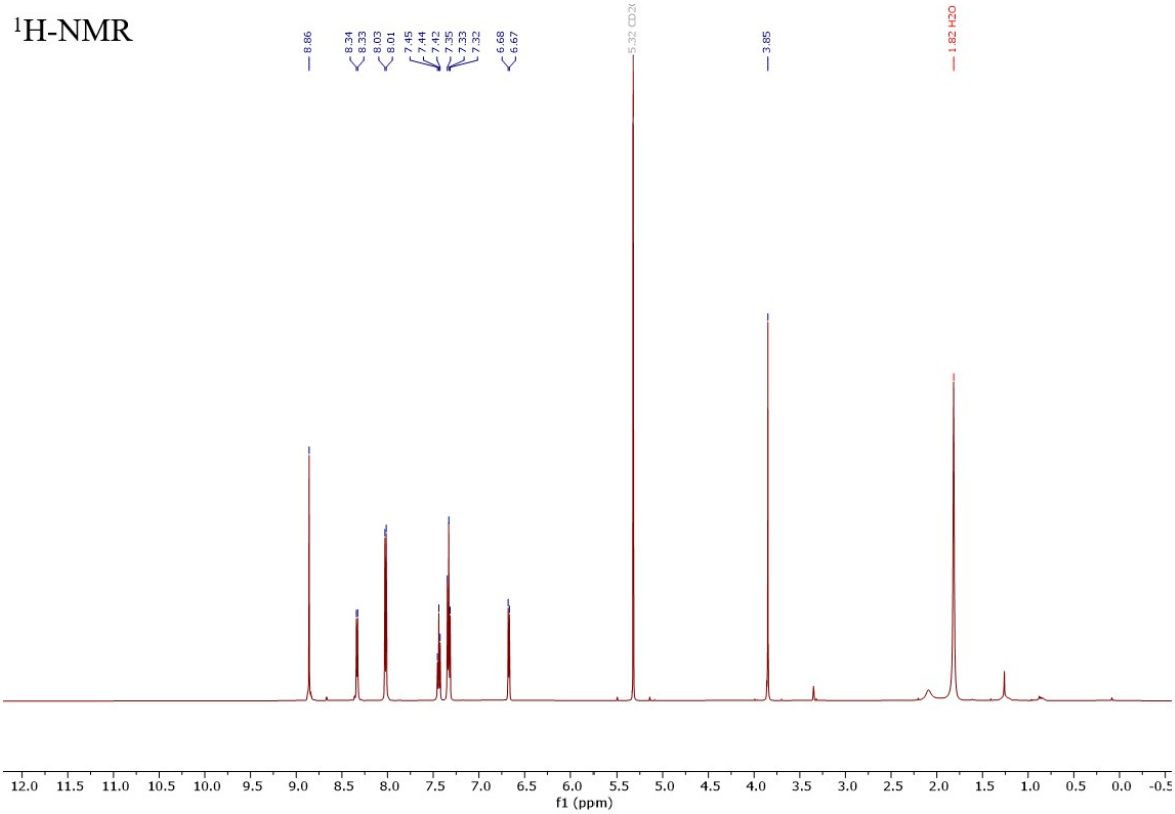

^{13}C-NMR

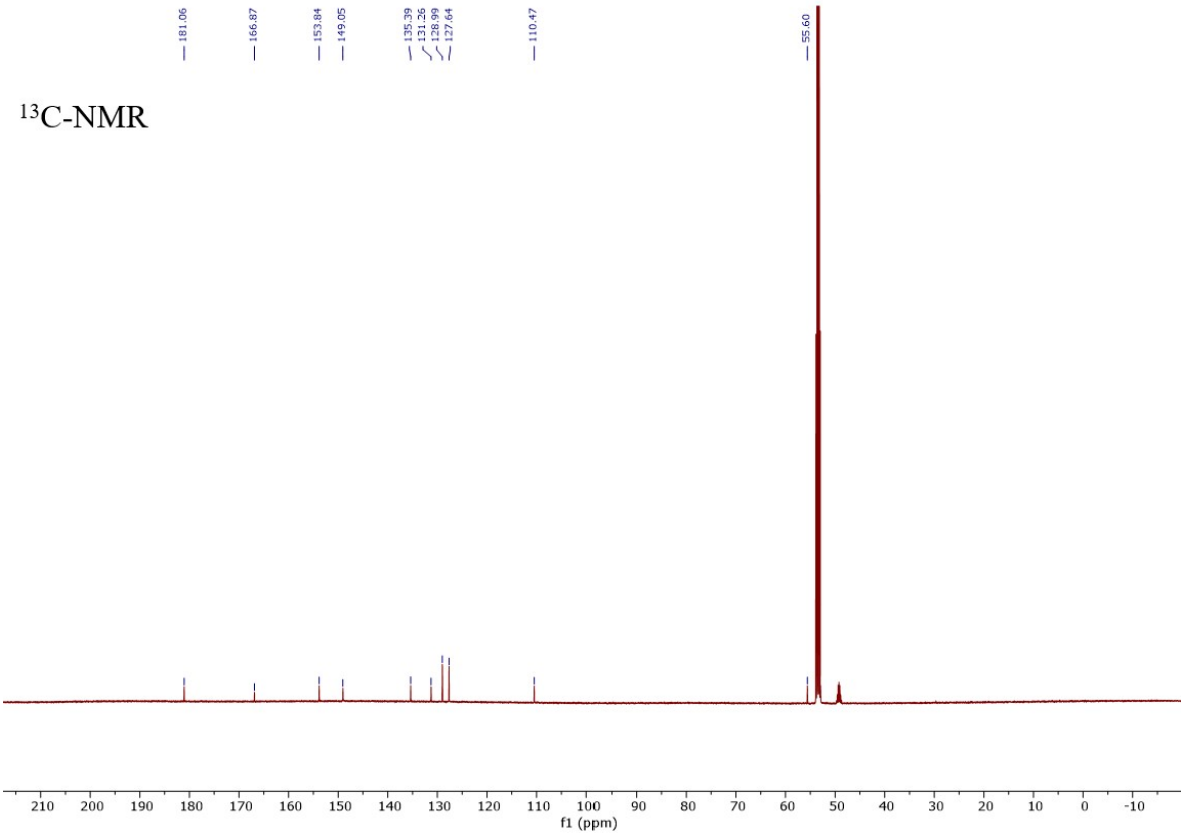

MeOPy-MeOBzO

^{1}H-NMR

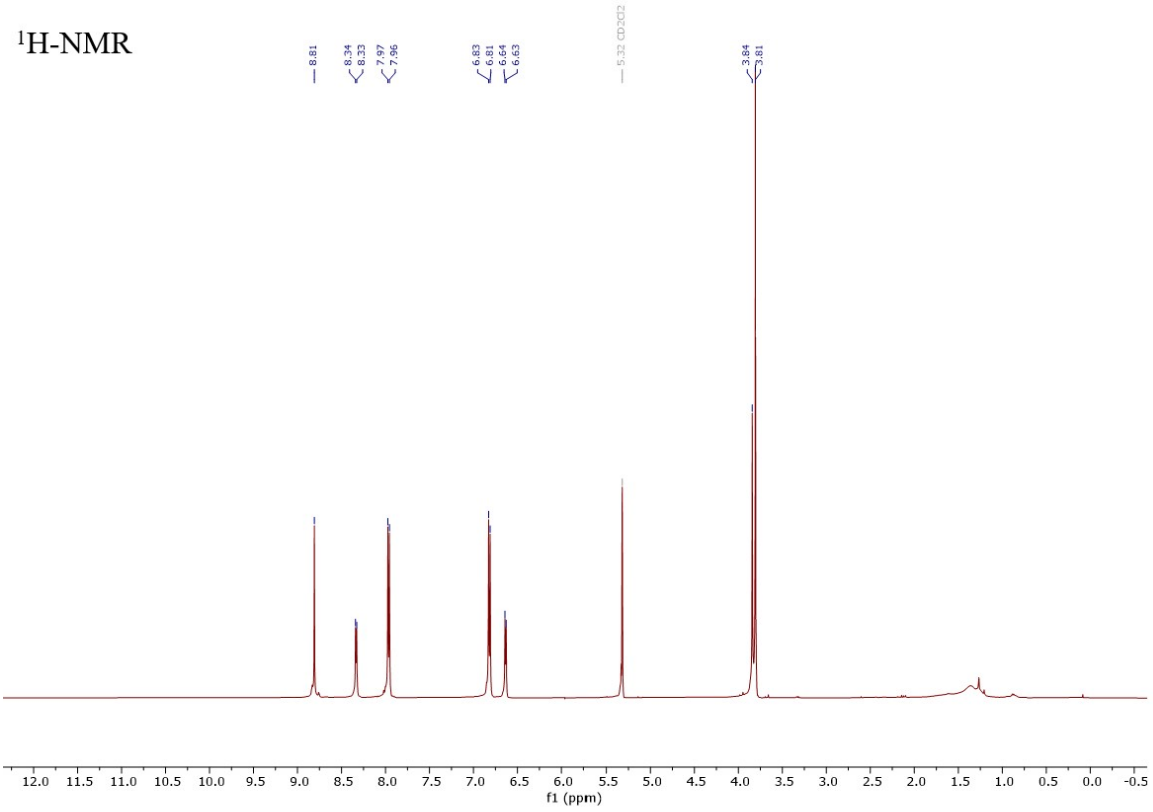

^{13}C-NMR

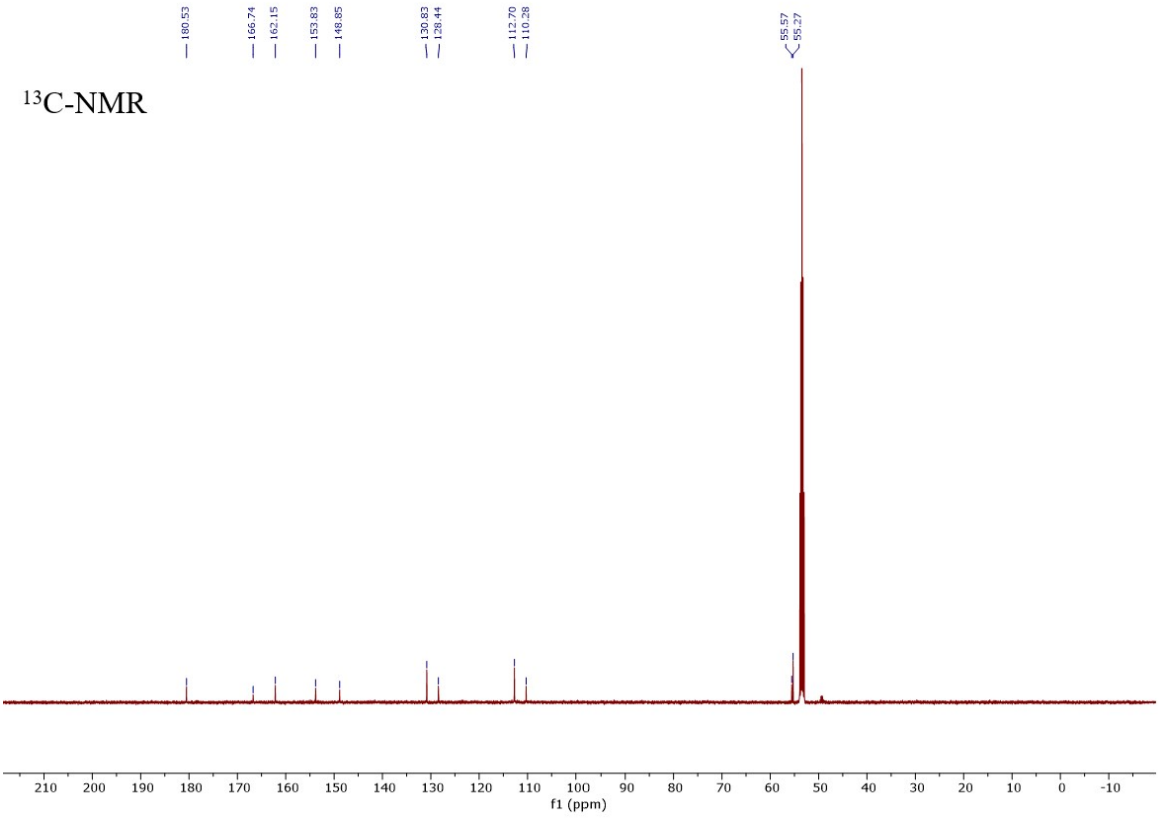

MeOPy-(MeO)$_3$BzO

^{1}H-NMR

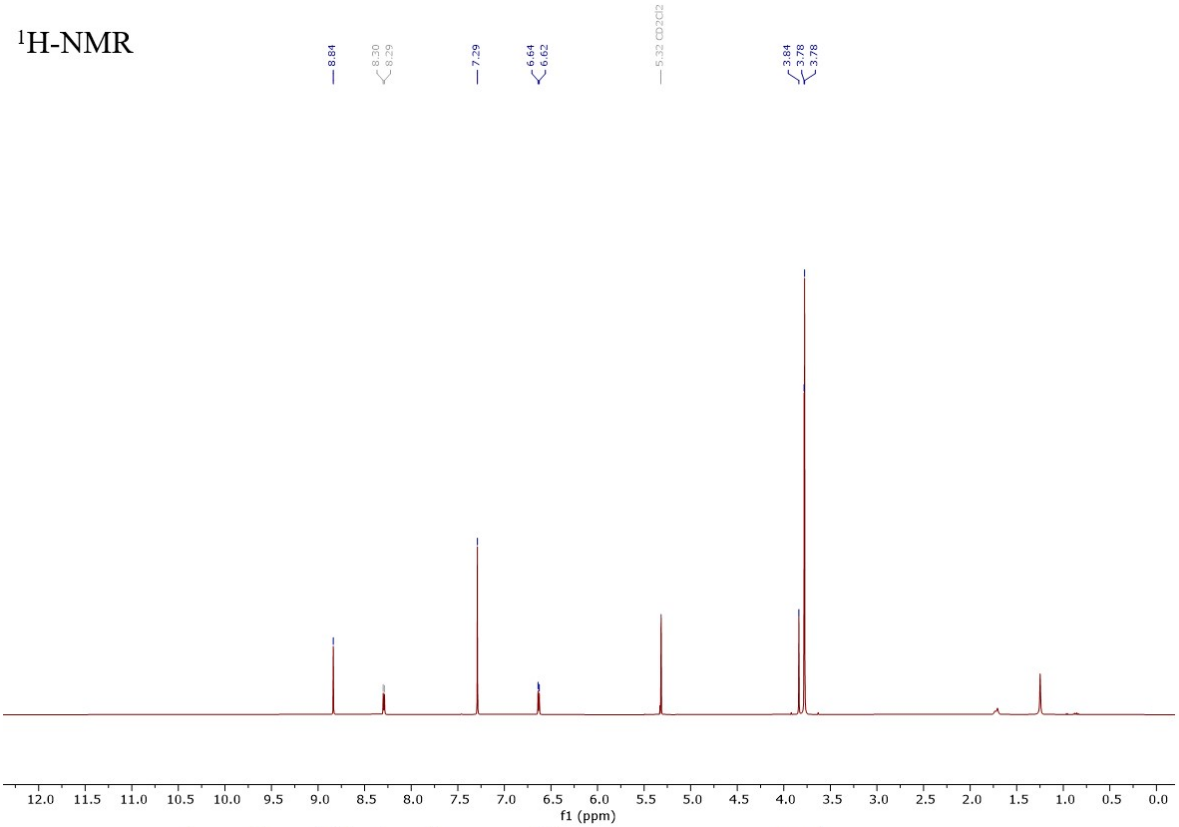

^{13}C-NMR

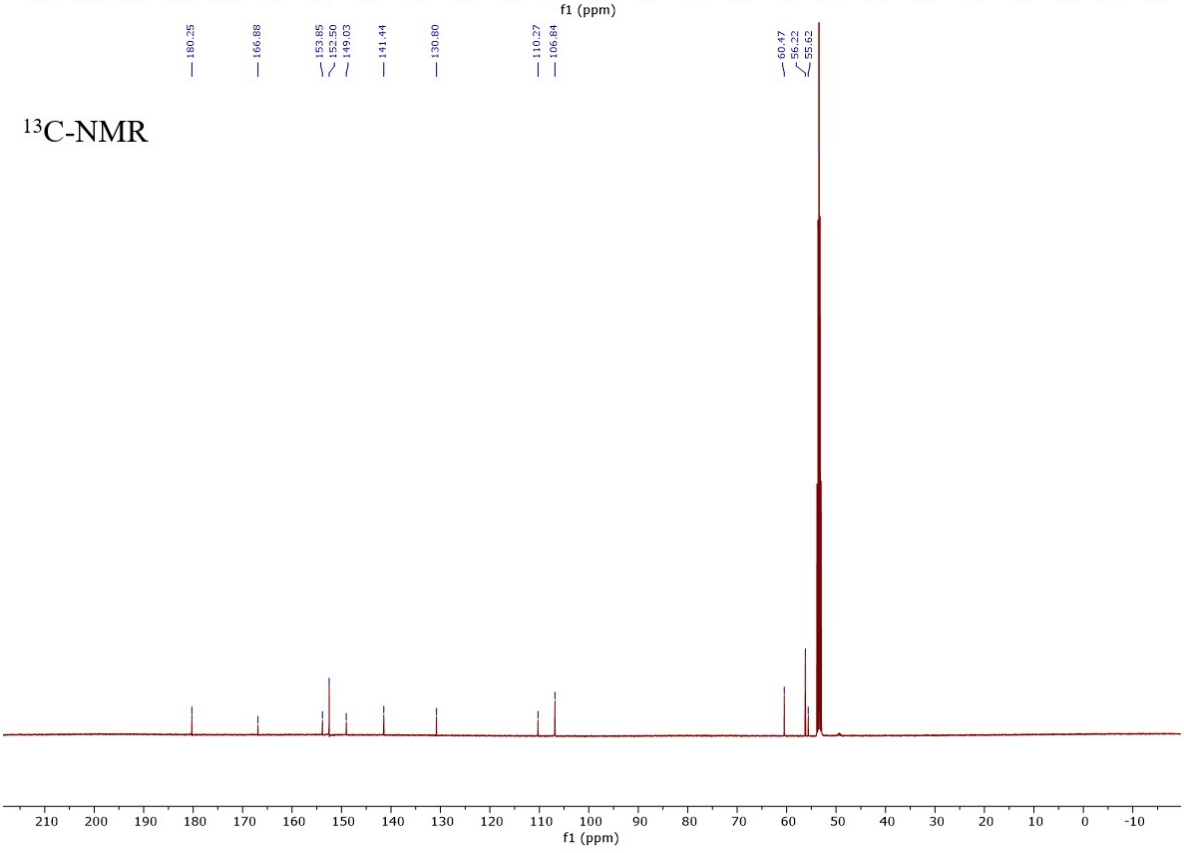

MePy-BzO

^{1}H-NMR

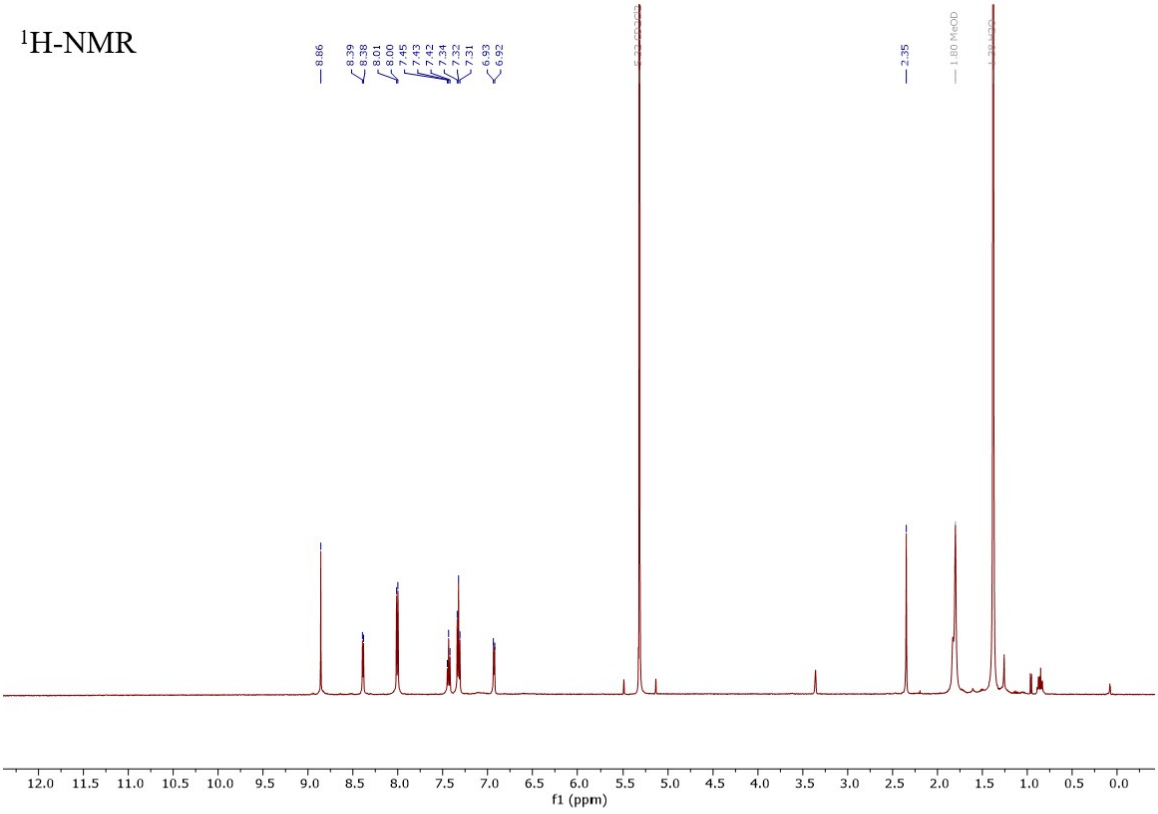

^{13}C-NMR

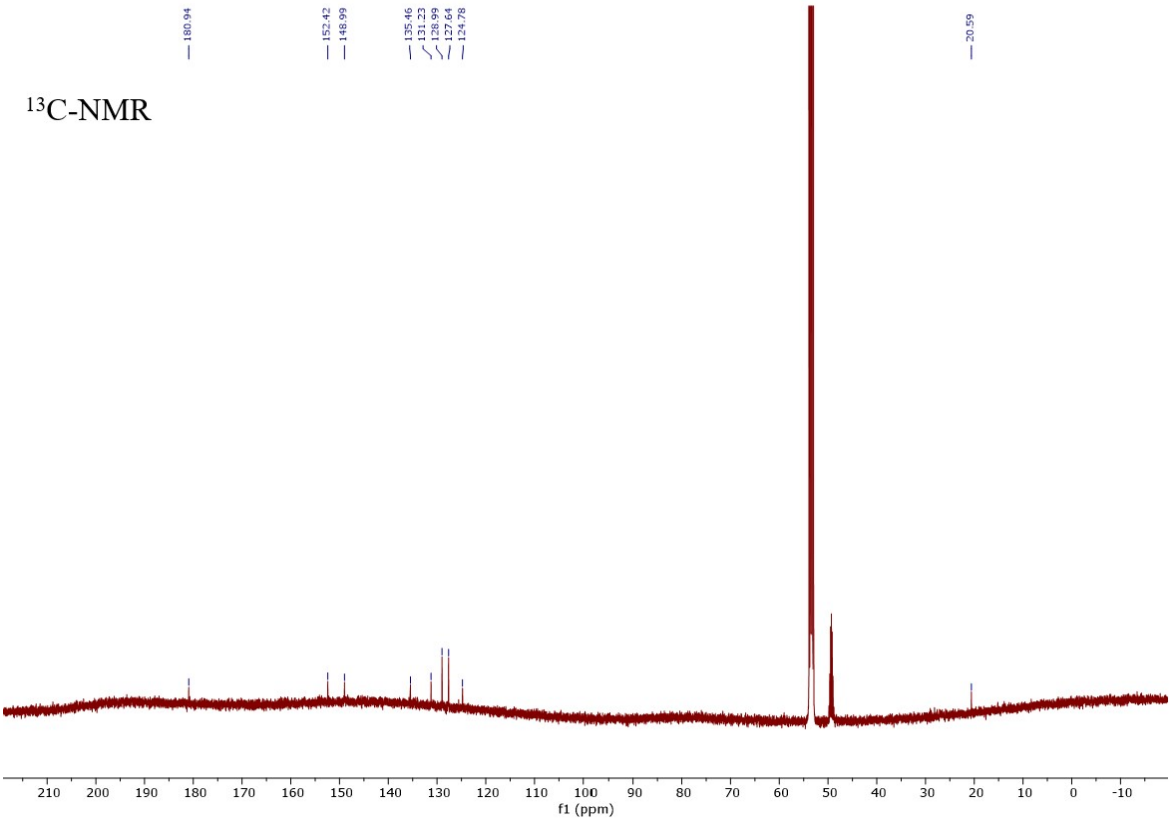

MePy-ClBzO

^{1}H-NMR

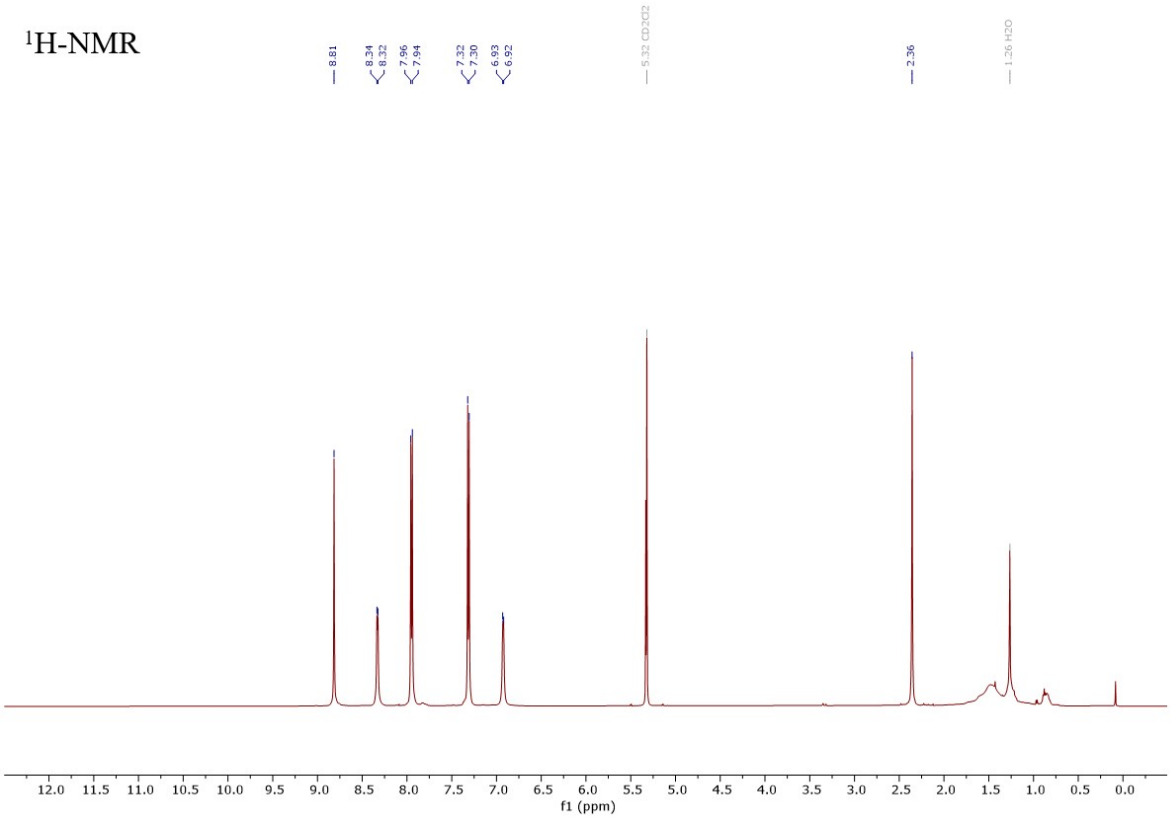

^{13}C-NMR

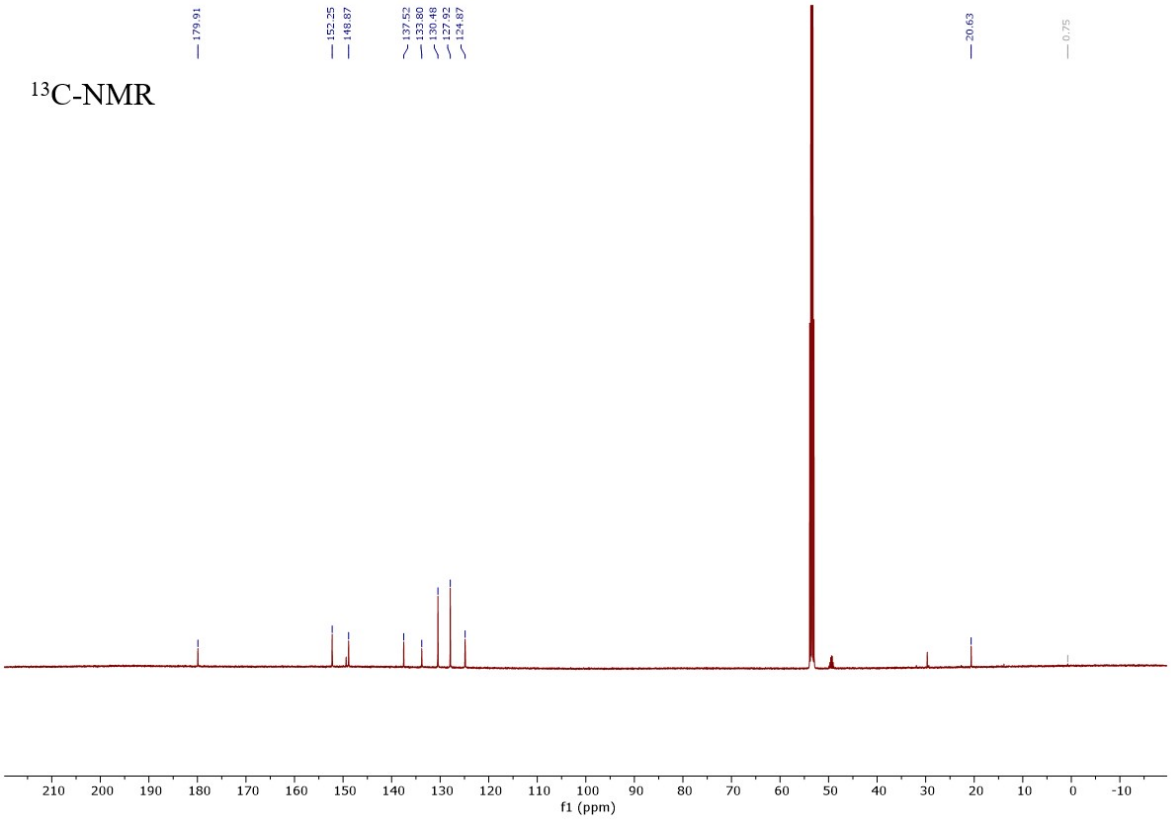

DOSY NMR Data

$Co_4O_4(OAc)_4$(4-methylpyridine)$_4$ mono-cubane

Fitted function:	f (x) = Io * exp (-D * x)
used gamma:	26752 rad/(s*Gauss)
used B values:	variable (gradient strength varied)
used little delta:	0.0010000 s
used big delta:	0.020000 s
Random error estimation of data:	RMS per spectrum (or trace/plane)
Systematic error estimation of data:	worst case per peak scenario
Fit parameter Error estimation method:	from fit using calculated y uncertainties
Confidence level:	95%
Used peaks:	automatically picked peaks
Used integrals:	area integral
Used Gradient strength:	all values (including replicates) used

Peak name	F2 [ppm]	offset	offsetError	Io	error	D [m2/s]	error	fitInfo
1	8.296	1.29e+07	1.838e+06	5.26e+09	1.679e+06	8.71e-10	7.547e-13	Done
2	6.952	1.51e+07	1.956e+06	5.41e+09	1.785e+06	8.68e-10	7.760e-13	Done

MePy-OAc

Fitted function:	f (x) = Io * exp (-D * x)
used gamma:	26752 rad/(s*Gauss)
used B values:	variable (gradient strength varied)
used little delta:	0.0010000 s
used big delta:	0.020000 s
Random error estimation of data:	RMS per spectrum (or trace/plane)
Systematic error estimation of data:	worst case per peak scenario
Fit parameter Error estimation method:	from fit using calculated y uncertainties
Confidence level:	95%
Used peaks:	automatically picked peaks
Used integrals:	area integral
Used Gradient strength:	all values (including replicates) used

Peak name	F2 [ppm]	offset	offsetError	Io	error	D [m2/s]	error	fitInfo
1	8.312	-1.34e+07	1.905e+06	3.44e+09	1.736e+06	6.45e-10	8.668e-13	Done
2	7.001	-1.35e+07	1.928e+06	3.39e+09	1.757e+06	6.43e-10	8.850e-13	Done

MePy-ClBzO

Fitted function:	f (x) = Io * exp (-D * x)
used gamma:	26752 rad/(s*Gauss)
used B values:	variable (gradient strength varied)
used little delta:	0.0010000 s
used big delta:	0.020000 s
Random error estimation of data:	RMS per spectrum (or trace/plane)
Systematic error estimation of data:	worst case per peak scenario
Fit parameter Error estimation method:	from fit using calculated y uncertainties
Confidence level:	95%
Used peaks:	peaks from peaklist.xml at spectrum
Used integrals:	area integral
Used Gradient strength:	all values (including replicates) used

Peak name	F2 [ppm]	offset	offsetError	Io	error	D [m2/s]	error	fitInfo
1	8.360	-4.03e+07	3.074e+06	6.39e+09	2.837e+06	5.74e-10	7.013e-13	Done
2	6.979	-2.33e+07	3.440e+06	7.07e+09	3.180e+06	5.78e-10	7.167e-13	Done

All DOSY measurements were collected at 298 K using a Bruker Ascend™ 400 MHz spectrometer equipped with a Bruker Avance IV NEO console and a diffusion probe (17 T/m max. gradient strength, capable of measuring diffusion rates down to 10^{-13} to 10^{-14} m^2/s). Measurements were recorded in 5% methanol-d_4 in CD_2Cl_2 at substrate concentrations of ~10 mM.

Comparing the diffusion rates of the $Co_4O_4(OAc)_4$(4-methylpyridine)$_4$ mono-cubane (8.68×10^{-10} m^2/s) and the **MePy-OAc** and **MePy-ClBzO** bis(cubanes), 6.43×10^{-10} m^2/s and 5.78×10^{-10} m^2/s respectively, corroborates the dimeric nature of the bis(cubanes) in solution.

Electrochemical Data

MePy-OAc-bipy

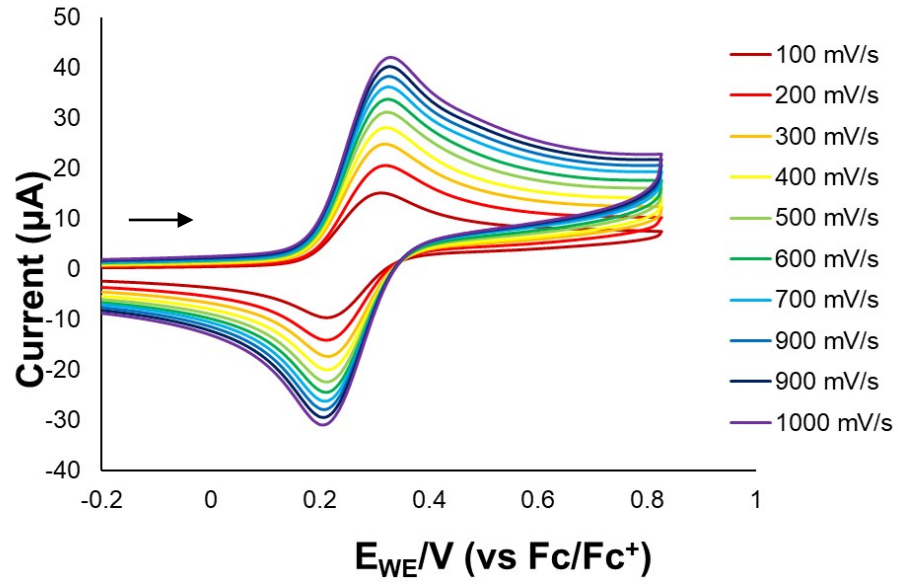

Fig S3. CV data for the **MePy-OAc-bipy** bis(cubane) collected with 100 mM [*n*-Bu_4N][$BArF_{20}$] in CH_2Cl_2 at various scan rates.

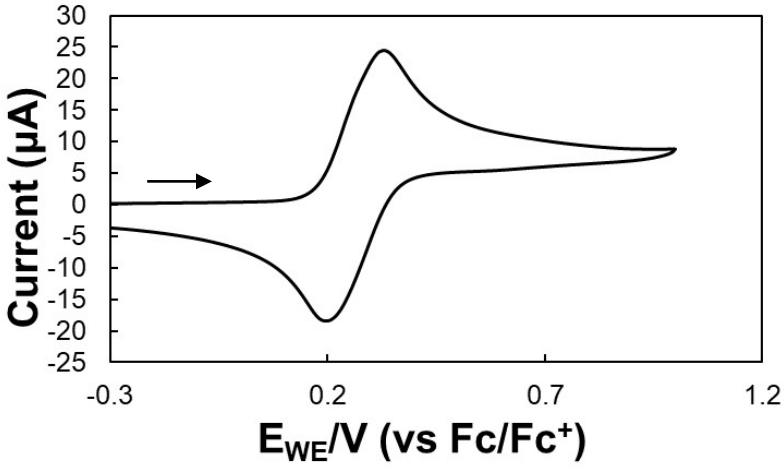

Fig S2. CV data for the **MePy-OAc-bipy** bis(cubane) collected with 250 mM [*n*-Bu_4N][PF_6] in CH_2Cl_2 at a scan rate of 100 mV/s.

MePy-OAc

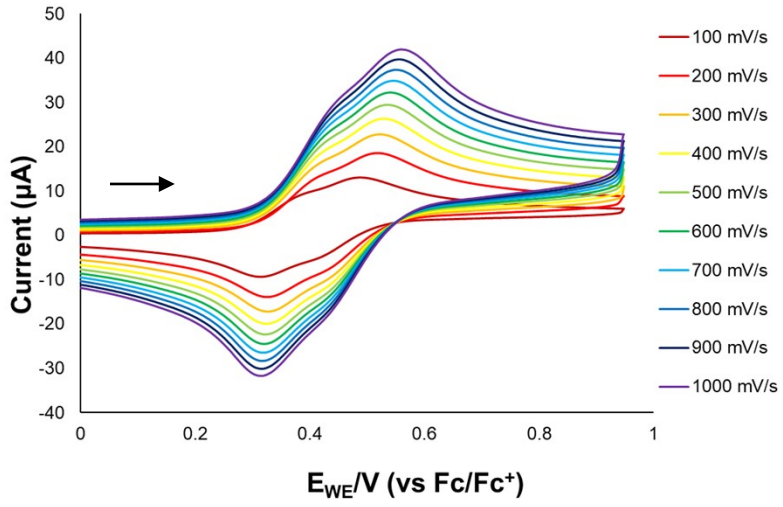

Fig S3. CV data for the **MePy-OAc** bis(cubane) collected with 250 mM [*n*-Bu_4N][PF_6] in CH_2Cl_2 at various scan rates.

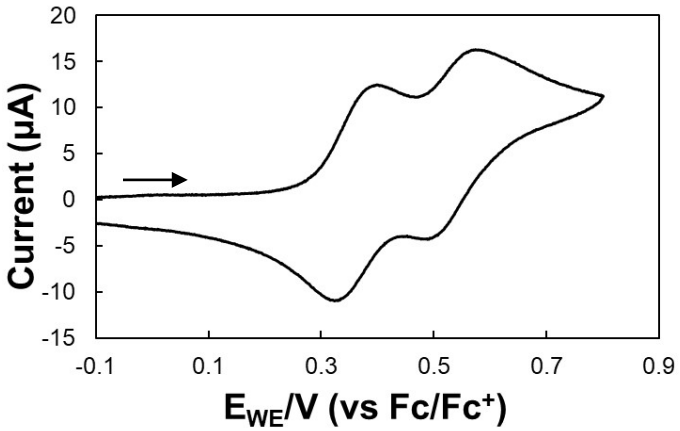

Fig S4. CV data for the **MePy-OAc** bis(cubane) collected with 100 mM [*n*-Bu_4N][$BArF_{20}$] in CH_2Cl_2 at a scan rate of 100 mV/s.

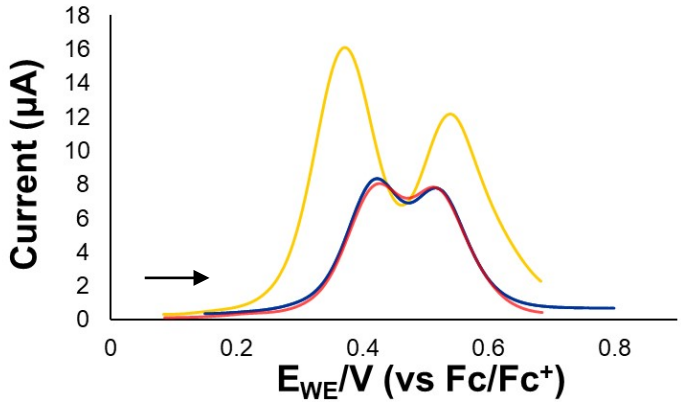

Fig S5. DPV data for the **MePy-OAc** bis(cubane) collected with 100 mM [*n*-Bu_4N][$BArF_{20}$] (gold trace), 250 mM [*n*-Bu_4N][PF_6] (blue trace), and 100 mM [*n*-Bu_4N][PF_6] (red trace) in CH_2Cl_2.

MeOPy-OAc

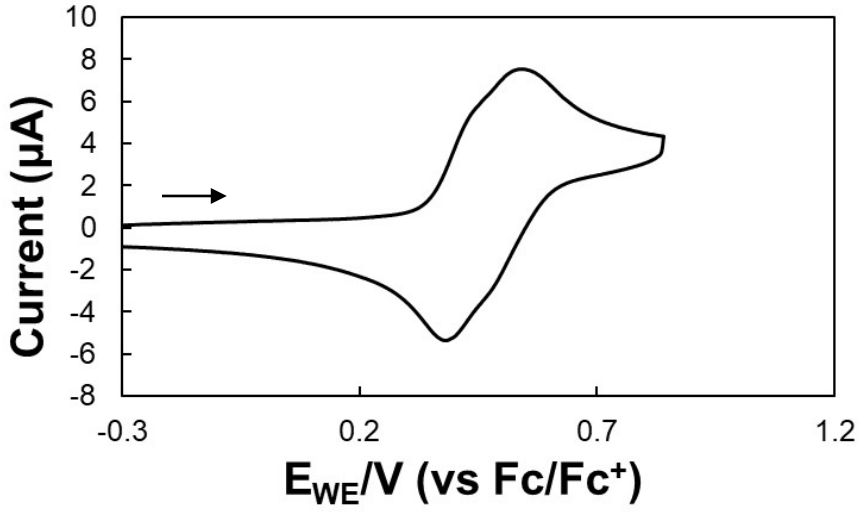

Fig S6. CV data for the **MeOPy-OAc** bis(cubane) collected with 250 mM [*n*-Bu_4N][PF_6] in CH_2Cl_2 at a scan rate of 100 mV/s.

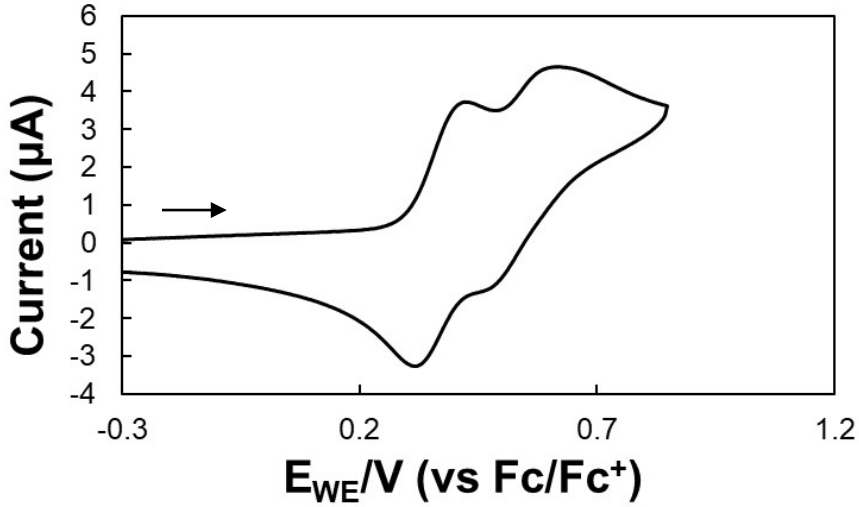

Fig S7. CV data for the **MeOPy-OAc** bis(cubane) collected with 100 mM [*n*-Bu_4N][$BArF_{20}$] in CH_2Cl_2 at a scan rate of 100 mV/s.

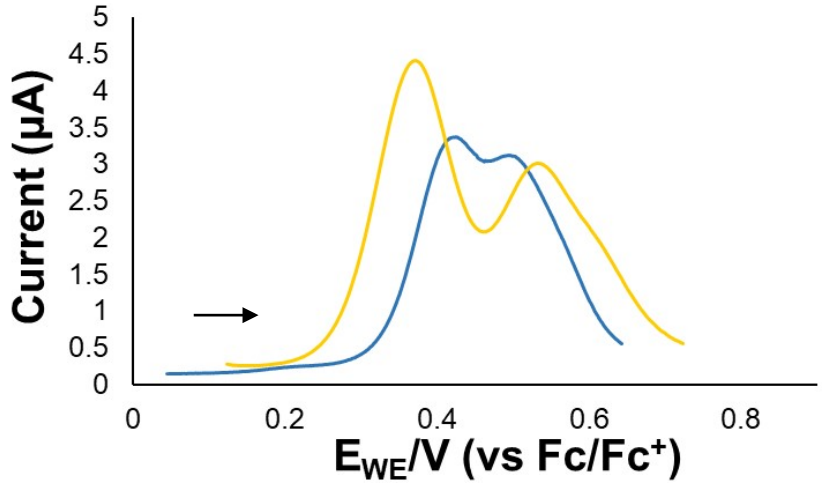

Fig S8. DPV data for the **MeOPy-OAc** bis(cubane) collected with 100 mM [*n*-Bu_4N][$BArF_{20}$] (gold trace) and 250 mM [*n*-Bu_4N][PF_6] (blue trace) in CH_2Cl_2.

DMAP-OAc

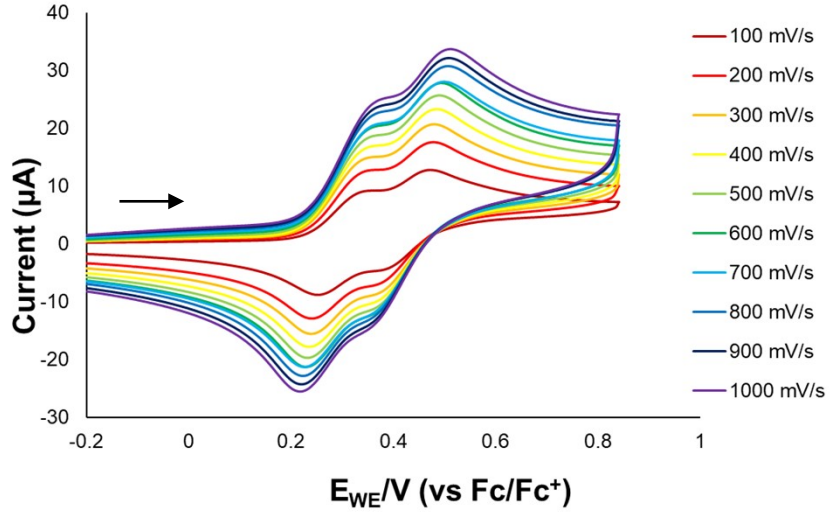

Fig S9. CV data for the **DMAP-OAc** bis(cubane) collected with 250 mM [*n*-Bu_4N][PF_6] in CH_2Cl_2 at various scan rates.

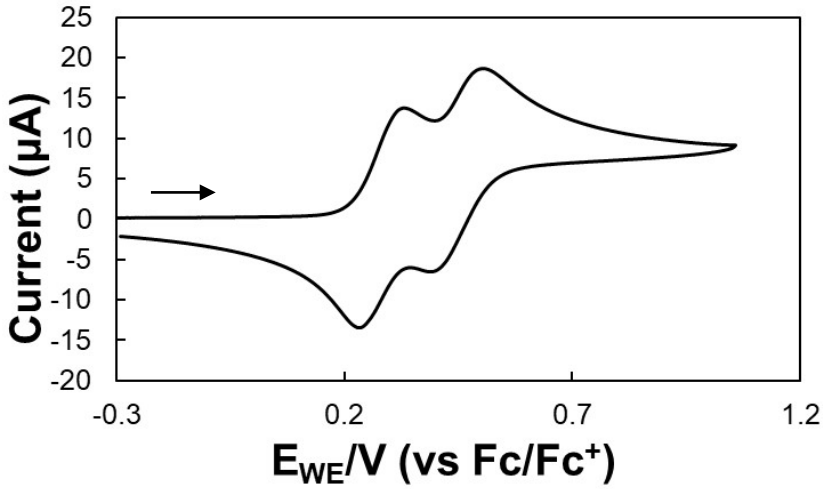

Fig S10. CV data for the **DMAP-OAc** bis(cubane) collected with 100 mM [*n*-Bu_4N][$BArF_{20}$] in CH_2Cl_2 at a scan rate of 100 mV/s.

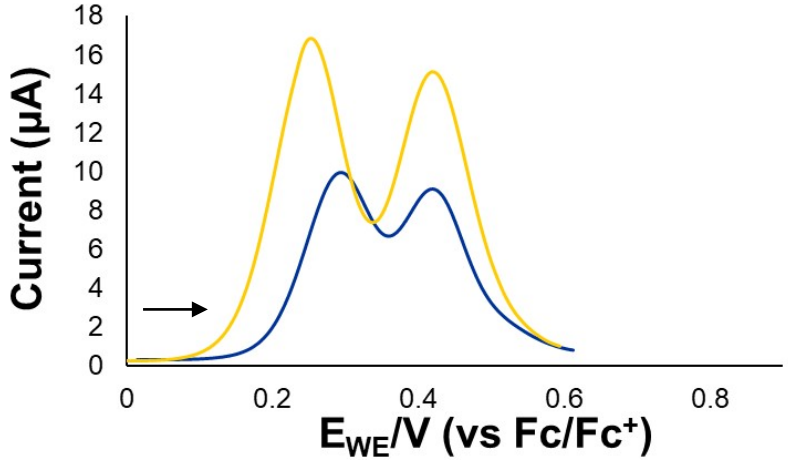

Fig S11. DPV data for the **DMAP-OAc** bis(cubane) collected with 100 mM [*n*-Bu_4N][$BArF_{20}$] (gold trace) and 250 mM [*n*-Bu_4N][PF_6] (blue trace) in CH_2Cl_2.

MeOPy-BzO

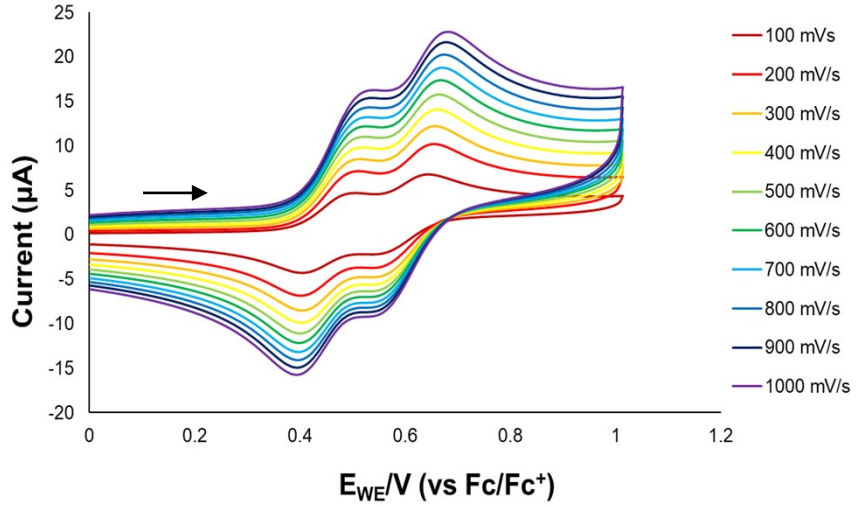

Fig S12. CV data for the **MeOPy-BzO** bis(cubane) collected with 250 mM [*n*-Bu_4N][PF_6] in CH_2Cl_2 at various scan rates.

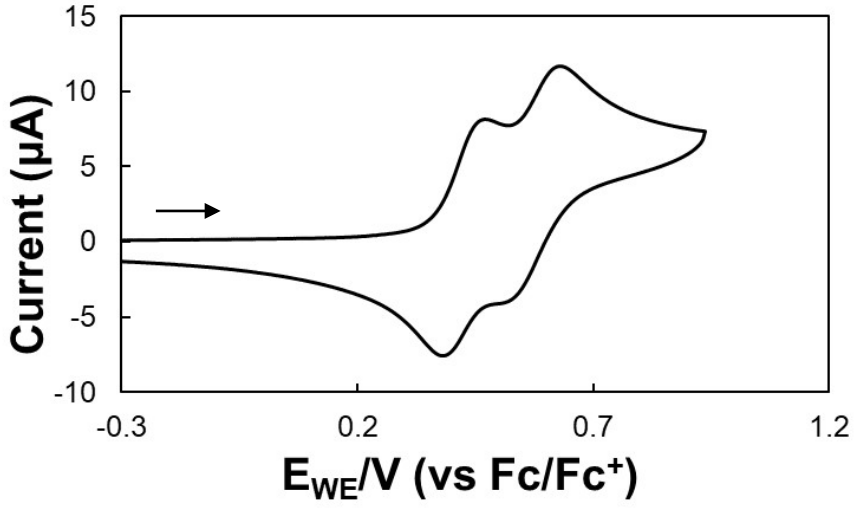

Fig S13. CV data for the **MeOPy-BzO** bis(cubane) collected with 100 mM [*n*-Bu_4N][$BArF_{20}$] in CH_2Cl_2 at a scan rate of 100 mV/s.

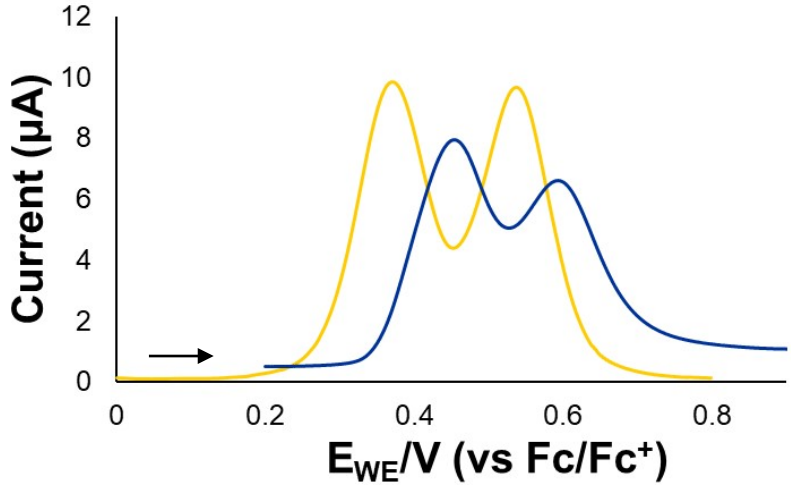

Fig S14. DPV data for the **MeOPy-BzO** bis(cubane) collected with 100 mM [*n*-Bu_4N][$BArF_{20}$] (gold trace) and 250 mM [*n*-Bu_4N][PF_6] (blue trace) in CH_2Cl_2.

MeOPy-MeOBzO

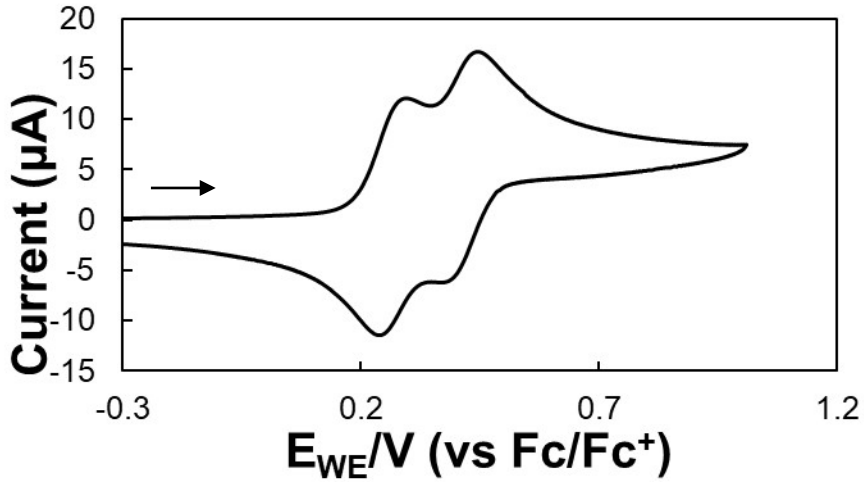

Fig S15. CV data for the **MeOPy-MeOBzO** bis(cubane) collected with 250 mM [*n*-Bu_4N][PF_6] in CH_2Cl_2 at a scan rate of 100 mV/s.

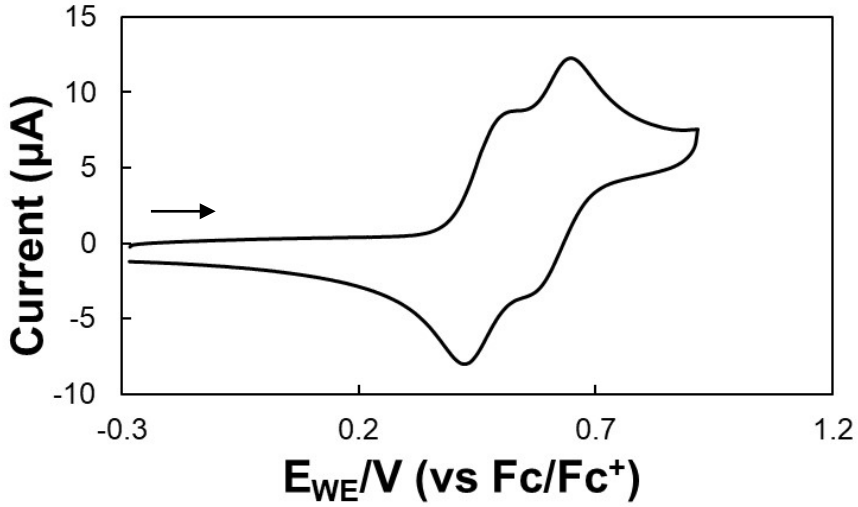

Fig S16. CV data for the **MeOPy-MeOBzO** bis(cubane) collected with 100 mM [*n*-Bu_4N][$BArF_{20}$] in CH_2Cl_2 at a scan rate of 100 mV/s.

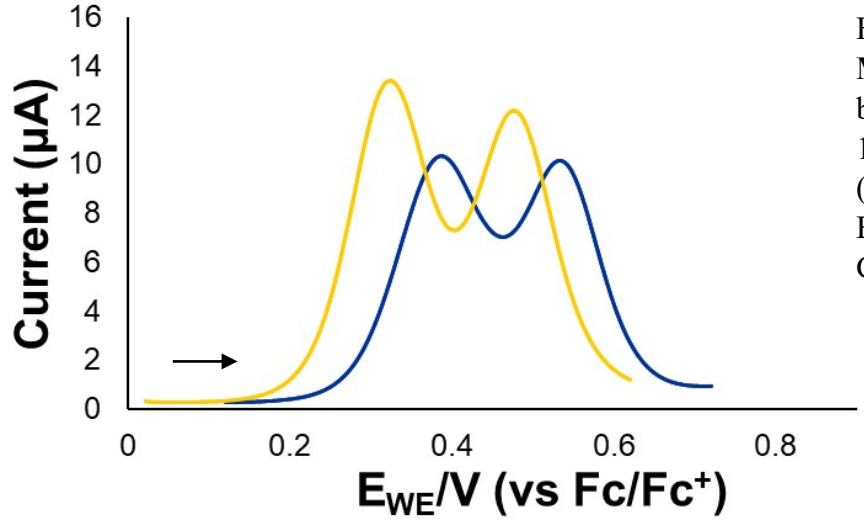

Fig S17. DPV data for the **MeOPy-MeOBzO** bis(cubane) collected with 100 mM [*n*-Bu_4N][$BArF_{20}$] (gold trace) and 250 mM [*n*-Bu_4N][PF_6] (blue trace) in CH_2Cl_2.

MeOPy-$(MeO)_3$BzO

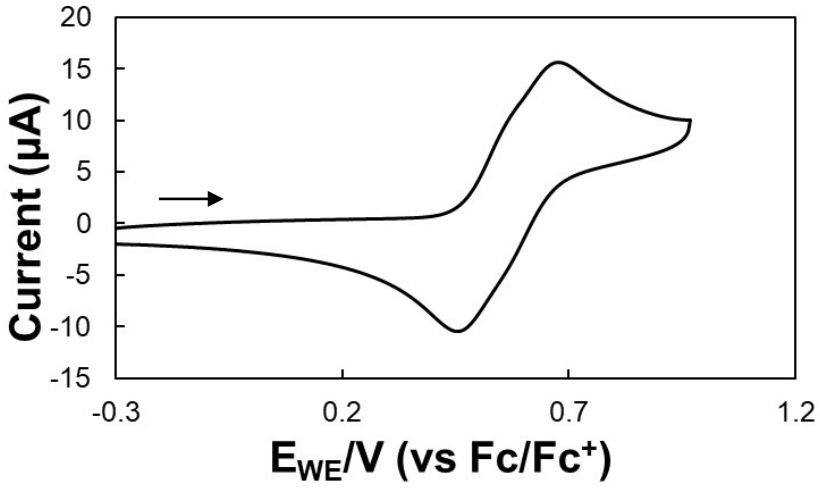

Fig S18. CV data for the **MeOPy-$(MeO)_3$BzO** bis(cubane) collected with 250 mM [*n*-Bu_4N][PF_6] in CH_2Cl_2 at a scan rate of 100 mV/s.

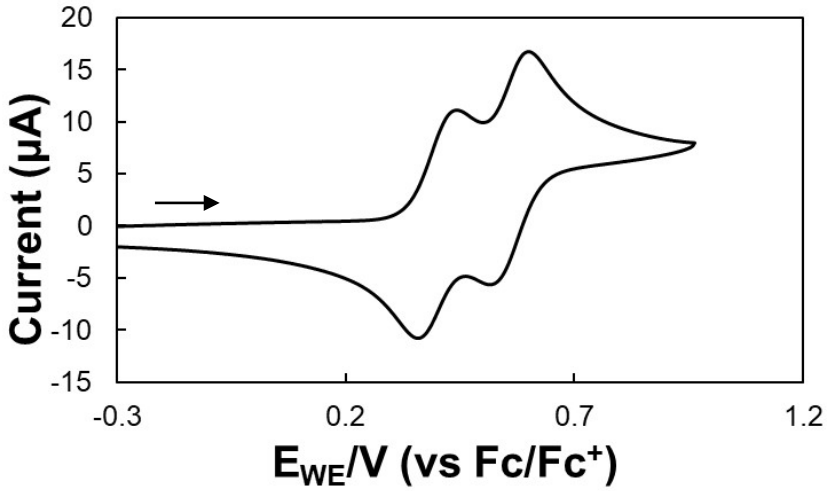

Fig S19. CV data for the **MeOPy-$(MeO)_3$BzO** bis(cubane) collected with 100 mM [*n*-Bu_4N][$BArF_{20}$] in CH_2Cl_2 at a scan rate of 100 mV/s.

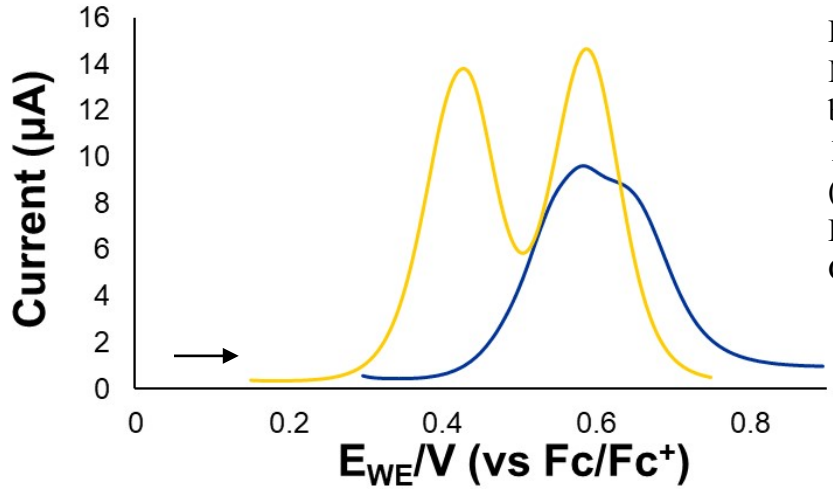

Fig S20. DPV data for the **MeOPy-$(MeO)_3$BzO** bis(cubane) collected with 100 mM [*n*-Bu_4N][$BArF_{20}$] (gold trace) and 250 mM [*n*-Bu_4N][PF_6] (blue trace) in CH_2Cl_2.

MePy-BzO

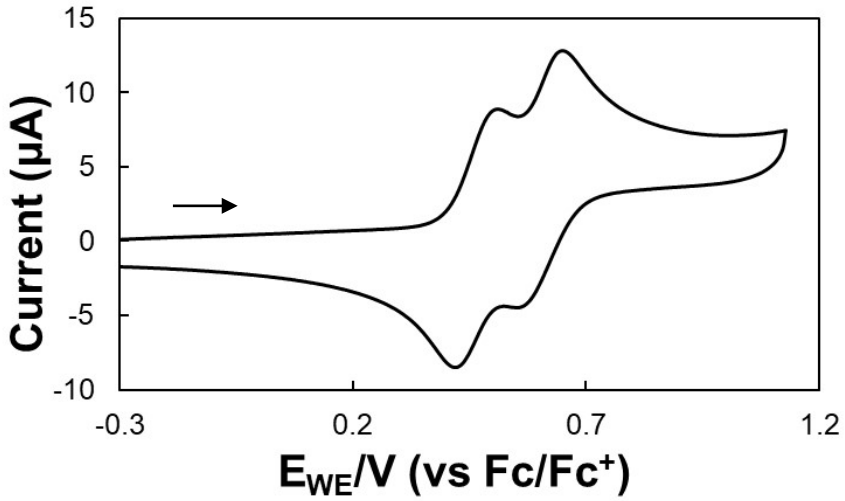

Fig S21. CV data for the **MePy-BzO** bis(cubane) collected with 250 mM [*n*-Bu_4N][PF_6] in CH_2Cl_2 at a scan rate of 100 mV/s.

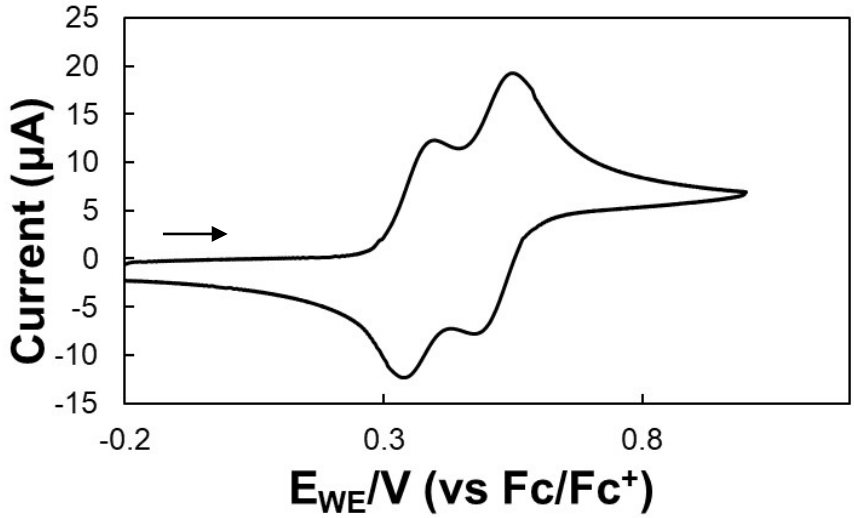

Fig S22. CV data for the **MePy-BzO** bis(cubane) collected with 100 mM [*n*-Bu_4N][$BArF_{20}$] in CH_2Cl_2 at a scan rate of 100 mV/s.

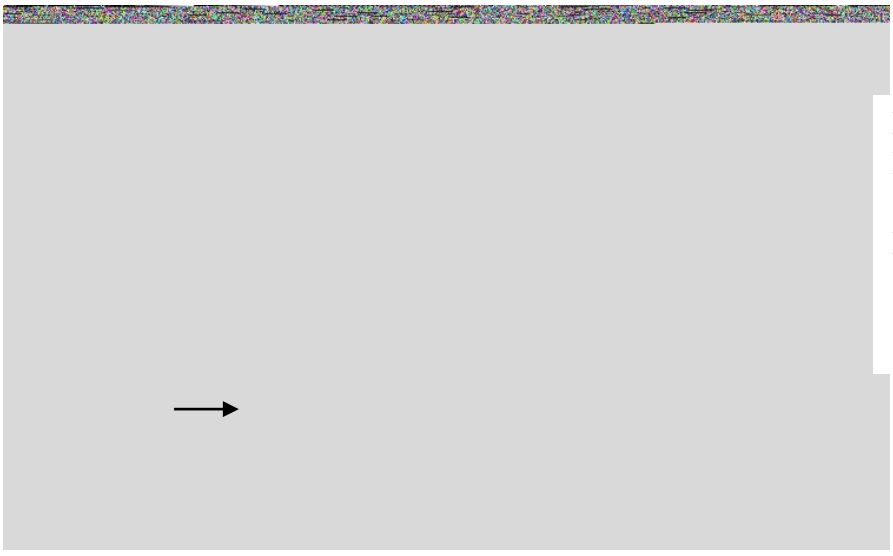

Fig S23. DPV data for the **MePy-BzO** bis(cubane) collected with 100 mM [*n*-Bu_4N][$BArF_{20}$] (gold trace) and 250 mM [*n*-Bu_4N][PF_6] (blue trace) in CH_2Cl_2.

MePy-ClBzO

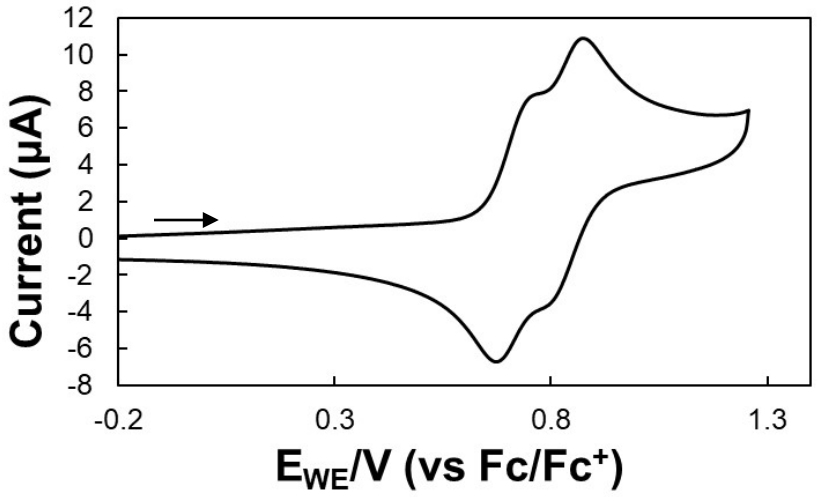

Fig S24. CV data for the **MePy-ClBzO** bis(cubane) collected with 250 mM [*n*-Bu_4N][PF_6] in CH_2Cl_2 at a scan rate of 100 mV/s.

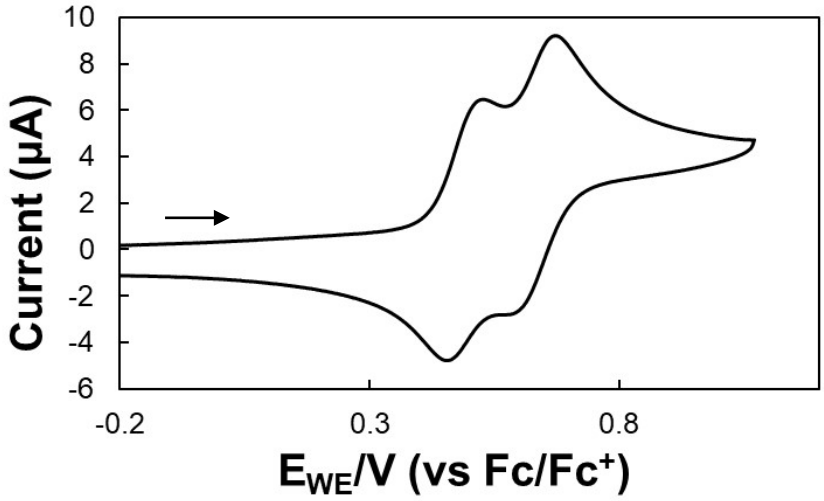

Fig S25. CV data for the **MePy-ClBzO** bis(cubane) collected with 100 mM [*n*-Bu_4N][$BArF_{20}$] in CH_2Cl_2 at a scan rate of 100 mV/s.

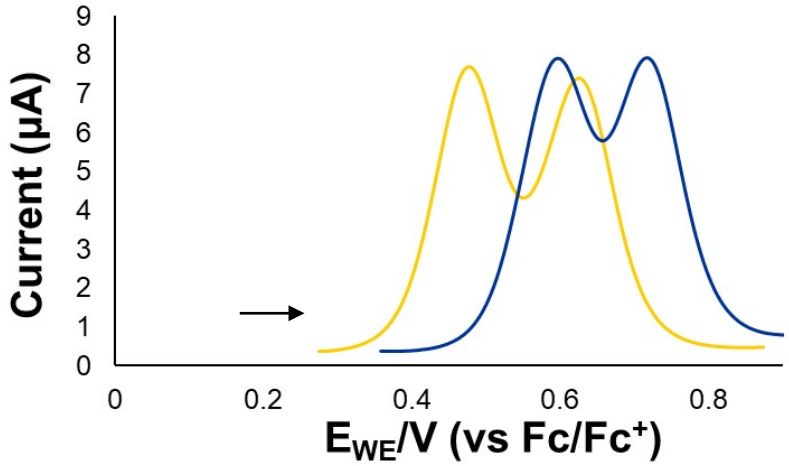

Fig S26. DPV data for the **MePy-ClBzO** bis(cubane) collected with 100 mM [*n*-Bu_4N][$BArF_{20}$] (gold trace) and 250 mM [*n*-Bu_4N][PF_6] (blue trace) in CH_2Cl_2.

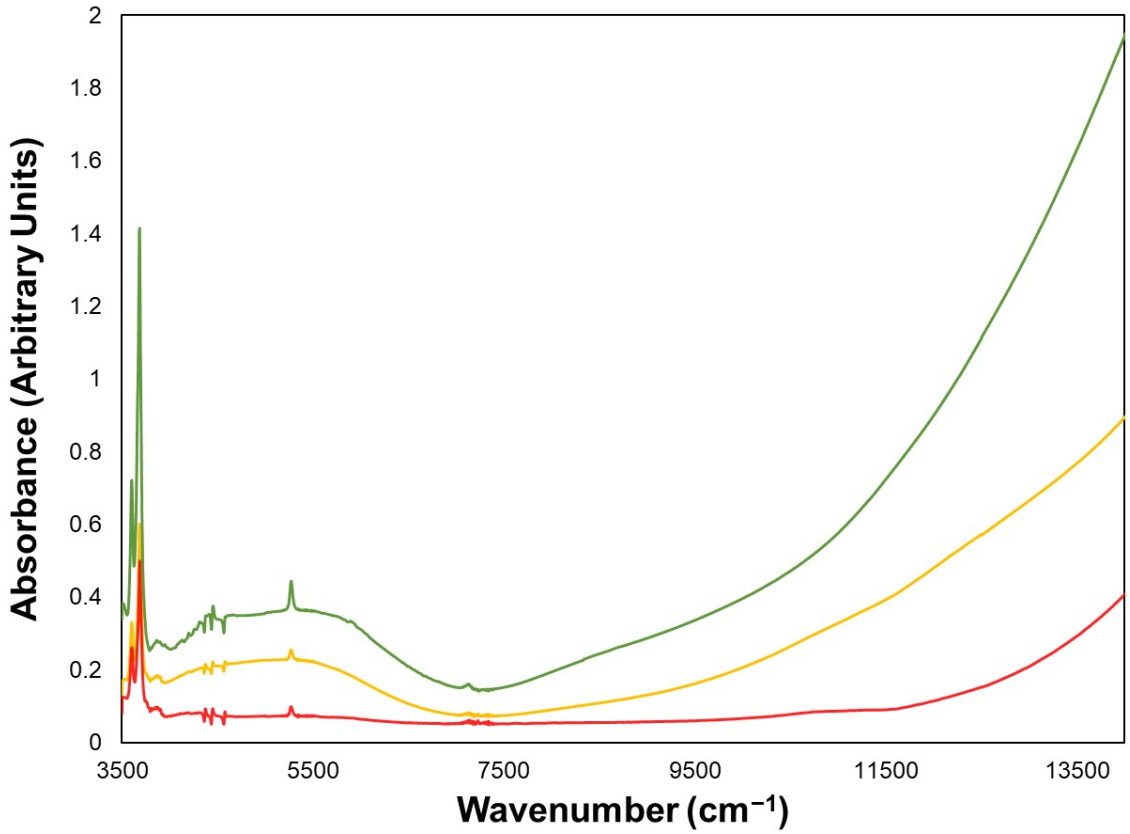

Fig S27. Spectroelectrochemistry of 10mM **DMAP-OAc** with 0.1 M [*n*-Bu_4N][PF_6] in CD_2Cl_2 at 0 mV vs silver wire (red trace), 600 mV vs silver wire (yellow trace), and 1 V vs silver wire (green trace). Spectral features are indistinguishable from those of the monocubane[5] and no inter-cubane IVCT bands could be identified.

References

(1) Chakrabarty, R.; Bora, S. J.; Das, B. K. Synthesis, Structure, Spectral and Electrochemical Properties, and Catalytic Use of Cobalt(III)−Oxo Cubane Clusters. *Inorg. Chem.* **2007**, *46* (22), 9450–9462. https://doi.org/10.1021/ic7011759.

(2) Nguyen, A. I.; Wang, J.; Levine, D. S.; Ziegler, M. S.; Tilley, T. D. Synthetic Control and Empirical Prediction of Redox Potentials for Co_4O_4 Cubanes over a 1.4 V Range: Implications for Catalyst Design and Evaluation of High-Valent Intermediates in Water Oxidation. *Chem. Sci.* **2017**, *8* (6), 4274–4284. https://doi.org/10.1039/C7SC00627F.

(3) Wheeler, T. A.; Tilley, T. D. Metal–Metal Redox Exchange to Produce Heterometallic Manganese–Cobalt Oxo Cubanes via a "Dangler" Intermediate. *J. Am. Chem. Soc.* **2024**, *146* (29), 20279–20290. https://doi.org/10.1021/jacs.4c05367.

(4) LeSuer, R. J.; Geiger, W. E. Improved Electrochemistry in Low-Polarity Media Using Tetrakis(Pentafluorophenyl)Borate Salts as Supporting Electrolytes. *Angewandte Chemie International Edition* **2000**, *39* (1), 248–250. https://doi.org/10.1002/(SICI)1521-3773(20000103)39:1%253C248::AID-ANIE248%253E3.0.CO;2-3.

(5) Brodsky, C. N.; Hadt, R. G.; Hayes, D.; Reinhart, B. J.; Li, N.; Chen, L. X.; Nocera, D. G. In Situ Characterization of Cofacial Co(IV) Centers in Co_4O_4 Cubane: Modeling the High-Valent Active Site in Oxygen-Evolving Catalysts. *Proc. Natl. Acad. Sci. U.S.A.* **2017**, *114* (15), 3855–3860. https://doi.org/10.1073/pnas.1701816114.